7

THE DEVELOPMENT OF A DYNAMIC ALGORITHM

7.1 INTRODUCTION

The traditional B-WIM approaches have limitations when the dynamic behaviour of the bridge-truck structural system does not follow a periodical oscillating pattern around the static response. These dynamic sources of inaccuracy are related to the excitation of the dynamic wheel forces by the bridge joint or a bump in the approach (Lutzenberger & Baumgärtner 1999). Inaccuracy can be high when measurement duration covers only a small number of natural periods of vibration (Peters 1984), or bridges have low first natural frequencies, or where significant dynamic amplification occurs. Low-pass filtering of the signal can be used to remove the effects of bridge vibration, but a significant part of the static response can be removed inadvertently (i.e., in the case of bridges with low natural frequencies, closely spaced axles and/or high vehicle speeds as seen in Section 3.5.1). This chapter describes the theoretical background of new B-WIM algorithms which allows for dynamics. The formulation of these algorithms is based on mathematical models described in Chapters 3 and 5. Their accuracy will be further tested in Chapters 8 and 9.

An algorithm based on spectral analysis of the strain signal has been developed by the author (González & O'Brien 1998) to reduce errors introduced through comparison of theoretical models and reality. The main novelties of this algorithm are the resolution of the problem in the frequency domain and the fully experimental calibration of the system (no theoretical reference to the bridge structural behaviour is required). However, the spectra are limited by the time the load is on the bridge and low frequency components could not be defined accurately in every case. Accordingly, while effective for vehicles with a low number of axles, this frequency domain approach failed to accurately predict the weights of a high number of axles.

Other research has focused on the development of dynamic algorithms in the time domain. These approaches try to correct the deviation from the static value that bridge and truck

dynamics could introduce in the measured strain (Dempsey et al. 1998b, O'Connor & Chan 1988a, 1988b). A new dynamic B-WIM algorithm that compares the measured strain to the theoretical total strain (instead of just the static) is presented. The equations of the total strain are made up of static and dynamic components. They can be derived from the mechanical characteristics of the bridge and the variables representing its general dynamic behaviour: natural frequencies, mode shapes and damping. Further dynamic modelling can be introduced through the application of optimisation techniques.

Most of these procedures yield a unique average load as a result of using the whole strain record at one longitudinal sensor location. This assumption could induce significant errors due to the varying applied force. Kealy and O'Brien (1998) extended the traditional static algorithm based on one sensor location to the use of several sensors along the length of the bridge. This approach has the advantage of providing the complete distribution of varying axle forces as the truck traverses the bridge and appears to reduce the effect of truck bouncing and rocking motions overall. However, it does not address the issue of bridge vibration which can result in significant errors for bridges with low natural frequencies. A dynamic multiple-sensor algorithm is developed here to overcome this problem (González et al. 1999). Finally, the multiple-sensor algorithm is extended to deal with simultaneous traffic events.

7.2 AN ALGORITHM BASED ON SPECTRUM ANALYSIS

All the B-WIM approaches to date calculate the weights in the time domain, this is, strain measurements from each scan are compared to corresponding theoretical values. As a result, final results are highly sensitive to truck location. In addition, a B-WIM algorithm based on a time-domain analysis depends on an accurate knowledge of the influence line and will tend to be sensitive to the dynamic characteristics of the trucks which are unknown. In this section, an alternative dynamic B-WIM system is presented based on a frequency spectrum approach. It utilises the frequency components of the strain signal and requires no prior knowledge of the influence line. The frequency domain representation of the signal, although entirely equivalent to the time domain representation, facilitates the suppression of high frequency effects and tends to reduce errors induced by speed measurement (this problem appears to have been overcome recently with optimisation techniques as described in Section 3.5).

7.2.1 Principle

This spectral algorithm is based on some properties of the Fourier Transform. If the measured strain at each scan n is $\varepsilon[n]$, the Fourier transform a_k for a frequency ($2*\pi*k/N$) is given by:

$$a_k = \frac{1}{N}\sum_{n=0}^{N-1} \varepsilon[n] * e^{-j2\pi Kn/N} \tag{7.1}$$

where N is the sample size, k the harmonic order and $j = \sqrt{-1}$. The bridge response due to a moving unit load can be represented in time or frequency domains as shown in Figure 7.1.

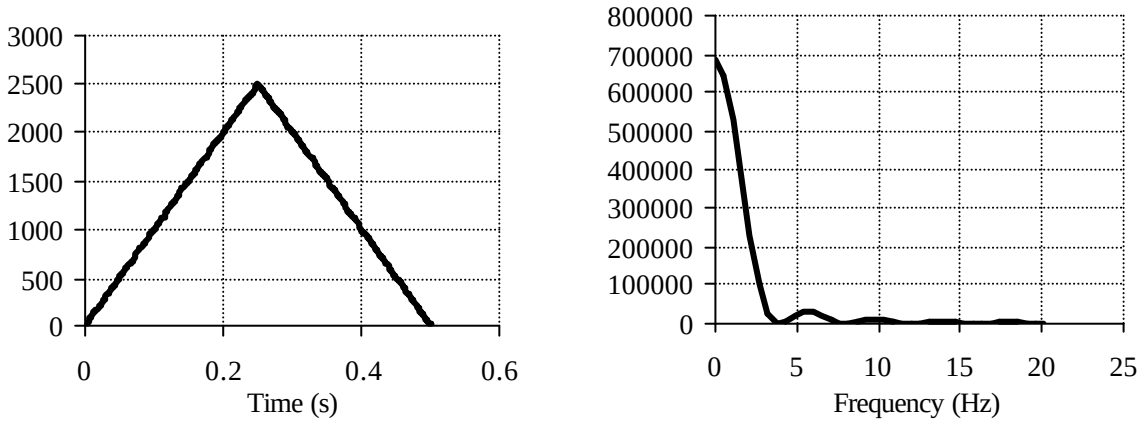

(a) Time Domain ($\varepsilon[t]$) (b) Magnitude in Frequency Domain ($|a_k|$)

Figure 7.1 – Bridge response due to a unit moving load

This transform has the property of linearity. If a load C times bigger acts on the bridge, the static strain response will be $C*\varepsilon[n]$, and then, the new magnitude of the Fourier transform for the k^{th} harmonic will be $C*a_k$. The phase component of the Fourier transform will remain the same.

If a signal is shifted by n_0 scans ($\varepsilon[n-n_0]$), the magnitude of the spectrum does not change, but the phase is different. The relationship between the transform of the shifted signal (b_k) and the original signal (a_k) is expressed by Equation 7.2.

$$b_k = a_k e^{-j\frac{2pkn_0}{N})} \tag{7.2}$$

Spectral energy can be expected to be concentrated around a period corresponding to the time it takes for a truck to cross the span. If the static response to two or more axles is considered, the total spectrum is a linear combination of their individual spectra.

The algorithm operates on the frequency-domain response of the bridge in free vibration and the frequency components of the strain signal, specifying which frequency range in the measured strain is to be suppressed. It compares results in the lowest frequency range, where most of the total energy of the signal is concentrated. Ideally this is far from the influence of the bridge's first natural frequency. When that frequency is excessively low, there will be spectral leakage that will have to be filtered out. Although there could be 'sidelobes' above the lowest frequencies containing significant energy due to the static response, this does not affect the algorithm's performance as the formulation operates in the frequency rather than the time domain. Accuracy depends on having a high definition of the response spectrum. Long flexible bridges allow for the collection of a lot of readings and a good definition of low frequency components, while short stiff bridges allow the extension of the algorithm to a wider range of frequencies.

7.2.2 Calibration

According to linearity and the time-shifting properties of Fourier transforms of digital signals, the total spectrum of the bridge response due to a calibration truck can be expressed as:

$$\overline{H_y}(f) = \overline{H_x}(f)[W_1 + W_2\, e^{(-jfn_1)} + ... + W_i e^{(-jfn_{i-1})} + ... + W_r e^{(-jfn_{r-1})}] \tag{7.3}$$

where

$\overline{H}_y(f)$: Spectrum of total strain,

$\overline{H}_x(f)$: Spectrum of the strain response due to a moving unit load,

W_i : Weight corresponding to axle *i*,

j : Imaginary number, i.e., $\sqrt{-1}$,

r : Number of axles,

n_i : Number of readings between the first axle and axle $(i+1)$,

f : Frequency, as $f = 2\pi k/N$, where k (0,1,2,..) represents the kth harmonic of the sample,

N : Number of strain readings induced by a vehicle crossing the bridge.

Figure 7.2 illustrates Equation 7.3 for a two-axle truck.

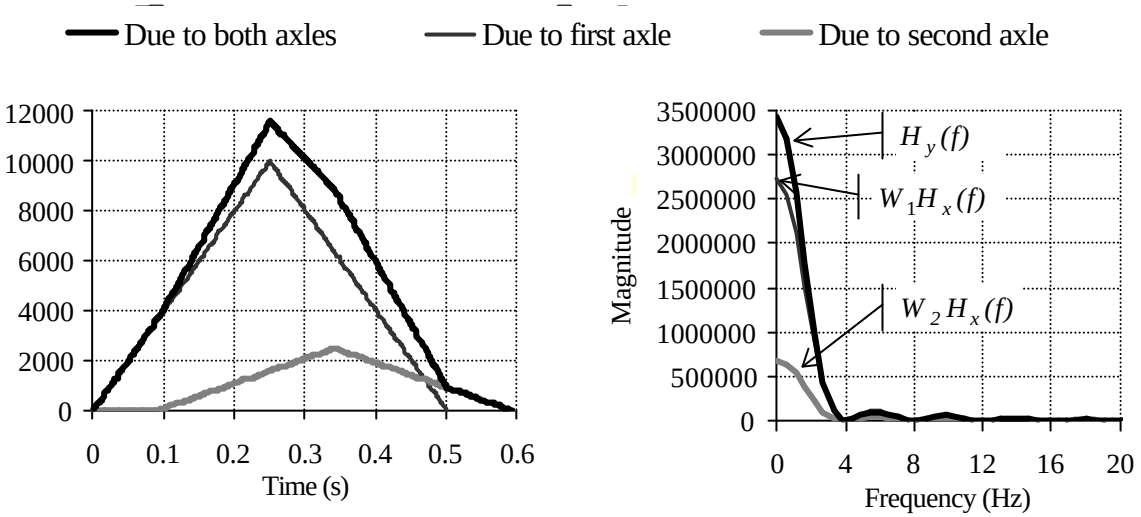

(a) Strain due to a two-axle truck (b) Spectra of (a)

Figure 7.2 – Calibration in frequency domain

As bridge frequencies and spectral leakage due to their components take place for relatively high frequencies, it is possible to assume for the lowest frequencies:

$$\overline{H}_y(f) \approx \overline{H}_m(f) \tag{7.4}$$

where $\overline{H}_m(f)$ is the spectrum of the measured strain.

Substituting Equation 7.4 in Equation 7.3, the spectrum corresponding to the pass of a single unit load can be obtained for the lowest frequencies by Equation 7.5:

$$\overline{H_x}(f) = \overline{H_m}(f) / [W_1 + W_2\, e^{(-jfn_1)} + \ldots + W_i e^{(-jfn_{i-1})} + \ldots + W_r e^{(-jfn_{r-1})}] \tag{7.5}$$

Very low speeds of the calibration truck allow for the collection of a lot of readings, and a good definition of low frequency components. A variety of speeds is necessary to evaluate the magnitude component of the fundamental harmonics for different sizes of the sample. Therefore, the scanning frequency should be quite high to reduce spectral leakage due to non-harmonic components. Some dispersion in spectra calculated through Equation 7.5 will occur due to truck dynamics.

7.2.3 Weight calculation

Once the spectrum of the bridge response due to a unit load is known, axles weights can be calculated by minimising an error function defined as the sum of squares of differences between the expected spectrum and the measured one, as follows:

Find W_i to minimise:

$$\sum_{f=0}^{f_c} [\overline{H_x}(f) \sum_{i=1}^{r} (W_i e^{(-jfn_{i-1})}) - \overline{H_m}(f)]^2 \tag{7.6}$$

where f_c is the limit frequency where spectra are compared. The spectrum $\overline{H_x}(f)$, taken as reference, must be the one corresponding to the speed of the traffic event being analysed. This spectrum can be calculated through inverse transform and interpolation from the calibration spectra obtained using Equation 7.5.

The error function is minimised by differentiating with respect to the weight of the k^{th} axle, W_k, which leads to the following expression:

$$\sum_{f=0}^{f_c} [\sum_{i=1}^{r} [W_i e^{(-j2\,fn_{i-1})} \overline{H_x}(f)] e^{(-jfn_{k-1})} \overline{H_x}(f)] = \sum_{f=0}^{f_c} [\overline{H_m}(f) \overline{H_x}(f) e^{(-jfn_{k-1})}] \tag{7.7}$$

In matrix form, the axle weights are given by Equation 7.8:

$$\{W\}_{rx1} = [H]_{rxr}^{-1} \{M\}_{rx1} \tag{7.8}$$

where the elements of the matrix of coefficients [*H*] are given by Equation 7.9 and the vector of independent terms {*M*} by Equation 7.10.

$$[H_{ik}] = \sum_{f=0}^{f_c} [e^{(-jf(n_{i-1}+n_{k-1}))} \overline{H_x}^2(f)] \tag{7.9}$$

$$\{M_k\} = \sum_{f=0}^{f_c} [\overline{H_m}(f)\overline{H_x}(f)e^{(-jfn_{k-1})}] \tag{7.10}$$

Spectra $\overline{H}(f)$ are composed of real and imaginary parts (or magnitude and phase). Axle weights are obtained from Equation 7.8 using complex arithmetic.

7.2.4 Theoretical Testing

A different number of trucks and road surface roughnesses are simulated to generate strains and the theoretical results used to check the validity of the algorithm. Pitch, bounce and roll of the truck body are taken into consideration. A beam model is used to represent the bridge. Road surface irregularities are idealised as a stochastic process and generated from power spectral density functions for 'very good', 'good', 'average' and 'poor' conditions (Wong 1993).

Results obtained by the new Spectral Bridge WIM approaches are compared to the conventional static approach, as described by Moses (1979). If a static bridge simulation is used to generate input strains, both algorithms are totally accurate. Further, if a bridge dynamic model consisting of constant forces moving at uniform speed is used, the spectral algorithm is still 100% accurate, unlike the static algorithm, where dynamics is a source of inaccuracy (even when this dynamic behaviour is linear).

Bridge-truck interaction model

The truck is represented by a planar 2-axle body, and implemented with the numerical methods proposed in Section 5.5. This planar model is represented in Figure 7.3. The bridge structure is modelled as a simply supported beam with surface irregularities. Bending strains are assumed to be measured at midspan.

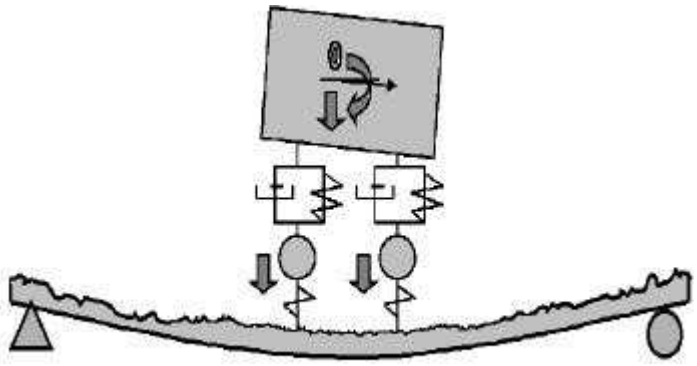

Figure 7.3 – Numerical approach

The features of the calibration truck, taken as reference, are: 50×10^3 kg.m^2 body inertia, 10×10^3 kg body mass equally distributed between axles, 4 m axle spacing, 20 m/s speed, and axle characteristics of: 1000 kg axle mass, 7×10^3 N.s/m suspension damping, 80×10^3 N/m suspension stiffness and 700×10^3 N/m tyre stiffness. The road conditions are taken as 'good'. The characteristics of the bridge model are: span 10 m, mass 12×10^3 kg/m, flexural rigidity 2.7×10^9 Nm^2, first natural frequency of the bridge in flexure 7.45 Hz and critical damping 5%. The road conditions are considered 'very good', unless otherwise specified.

Effect of different parameters

For any Bridge WIM system, based on static or dynamic principles, there is a difficulty in obtaining an accurate system calibration. In static terms, the calibration consists of determining an accurate influence line for the bridge. This is often determined by scaling and/or adjusting a theoretical influence line to give a best fit of measured to theoretical results for the calibration vehicle. For a dynamic algorithm, an attempt can be made to characterise the bridge in a similar way. However, the characteristics thus found tend to be highly dependent on the properties of the truck used for the calibration process. In this section, the sensitivity of the results to the differences in the properties of the truck being weighed and those of the calibration vehicle are investigated.

Influence of road conditions

There are clearly greater amplitudes of dynamic wheel forces in poor road conditions than in good conditions. Therefore, truck initial conditions have a strong influence on final results and the average axle load on the bridge could have an important deviation from the

static value. The dynamic algorithm is less sensitive to this variation than the static one. If the truck was calibrated in average road conditions, the maximum error in axle weight when half loaded is 2.75% if adopting the traditional approach compared to 1.47% with the dynamic one. However, this finding is based on a stochastic representation of the profile and does not take account of any biases that might be introduced by such phenomena as spatial repeatability (O'Connor et al. 1999).

Influence of bridge parameters

If inertia is decreased or span length/mass increased, the value of the natural frequencies will be reduced, and bridge-truck interaction will take place at lower frequencies. The difference between the total and static answers then becomes greater, and the dynamic algorithm is less sensitive to this variation than the static one.

Influence of vehicle parameters

Figure 7.4 shows the relationship between bending moment and truck position for a two-axle truck and the corresponding Fourier transform for the static and total (static + dynamic) cases. The response spectrum for frequencies below 5 Hz is very close for the two cases. By applying the new algorithm in this frequency range, the increasing deviation due to truck and bridge interaction at higher frequencies is avoided. The results of Figure 7.4 have been used to calibrate both systems for the comparisons described in this section.

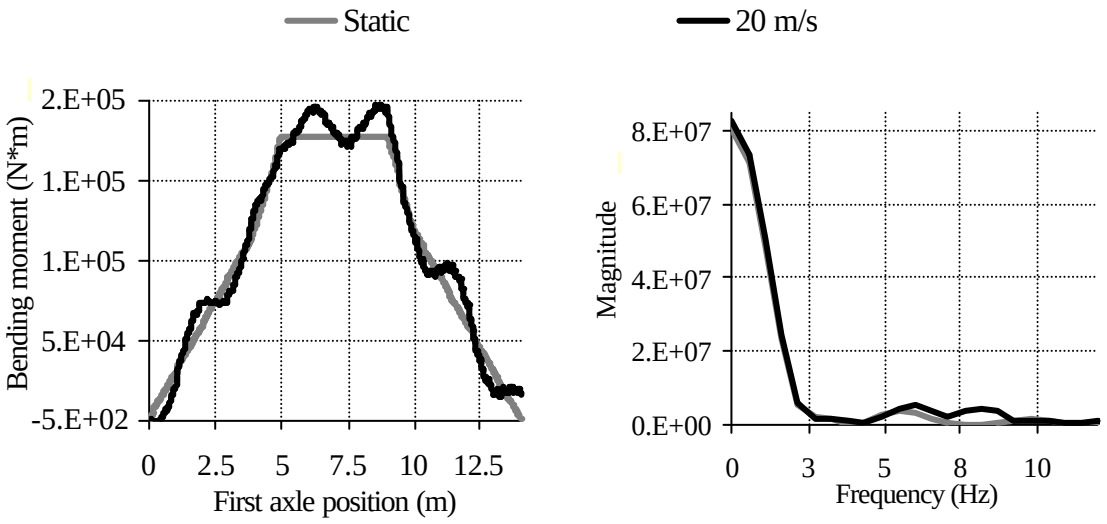

(a) Moment versus vehicle position (b) Spectra response

Figure 7.4 – Static and total bending moment for a two-axle truck

For the new system, values of the 'measured' spectra corresponding to a moving unit load can be obtained through Equation 7.5. Then, weights are calculated using Equation 7.8. There is an increasing deviation between the static and the total bending moment response with increasing speed but this increase ends at a certain speed.

Figure 7.5(a) gives the maximum relative error in individual axle weights for both the static and the new algorithms due to differences in the axle spacing and the position of the centroid of the body mass between sample truck and calibration truck. Figure 7.5(b) compares this maximum error when there are differences in the sprung and unsprung masses. The relative error due to a difference in the position of the sprung mass between the calibration truck and the truck being weighed is quite significant as illustrated in Figure 7.5(a). A difference in axle spacing can be seen to be an important source of inaccuracy for the spectral algorithm. Accuracy is also sensitive to mass differences as can be seen in Figure 7.5(b). This sensitivity has been found to be greater when the sprung or unsprung frequency is lower. Although the new algorithm gives an improvement in the accuracy of individual axle weights over the conventional static bridge WIM algorithm, the degree of uncertainty introduced by vehicle parameters is still important and truck low frequencies might yield an average value far from the static one in short span bridges.

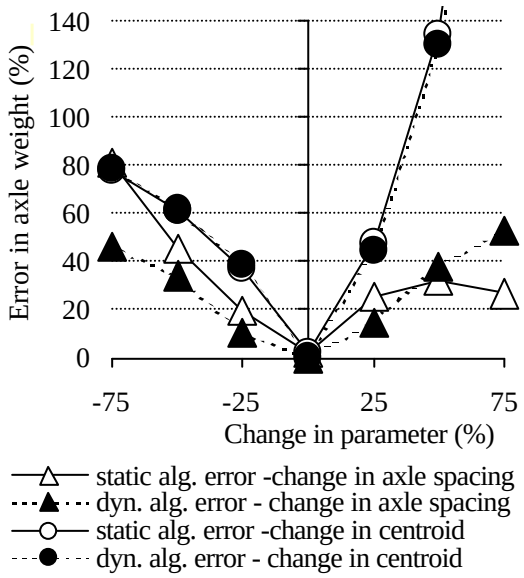

(a) Relative error due to change in axle spacing or centroid of sprung mass

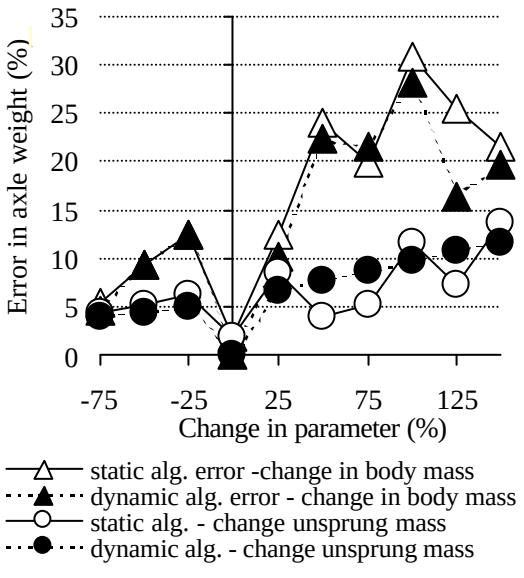

(b) Relative error due to change in vehicle masses

Figure 7.5 - Effect on accuracy of the change of vehicle masses and distances

In the same way, the influence on accuracy of vehicle mechanics is illustrated in Figure 7.6. Figure 7.6(a) shows the effect of a difference in pitch inertia or suspension damping while Figure 7.6(b) shows the effect of a difference in tyre or suspension stiffness. In these figures the dynamic algorithm is generally better than the static algorithm.

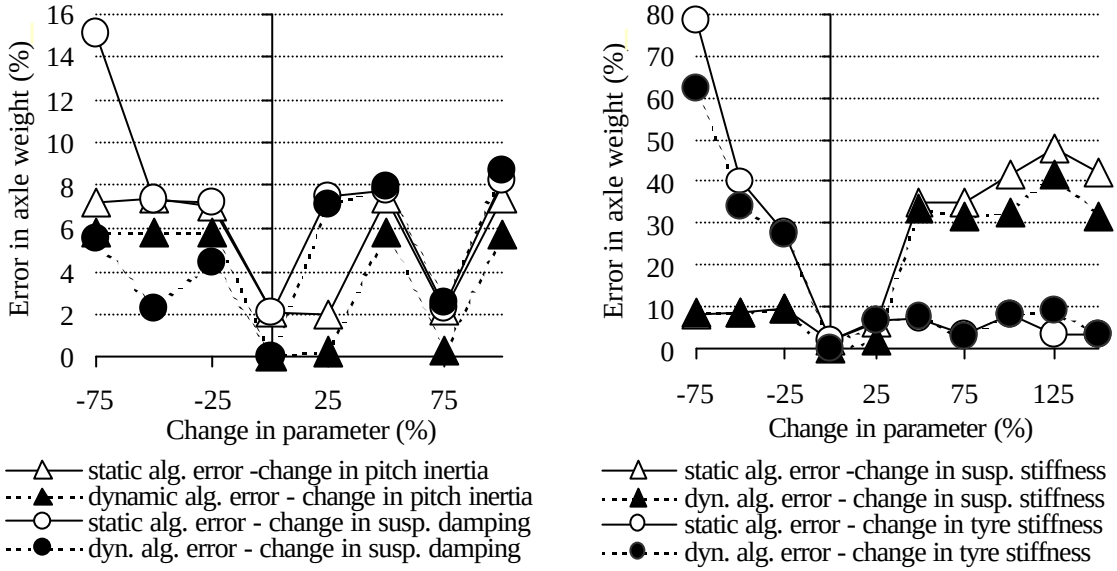

(a) Relative error due to change in pitch inertia/Damping

(b) Relative error due to change in tyre/suspension stiffness

Figure 7.6 – Effect on accuracy of the change of suspension and tyre characteristics

7.2.5 Advantages and Disadvantages

A Bridge WIM system gives a continuous reading that allows for a frequency domain analysis. In addition,

- Sources of inaccuracy in traditional static approaches are: (a) The determination of the real influence line; (b) An exact location of the truck on the bridge at each instant, (c) dynamics of bridge and truck introducing a deviation from the static response and (d) Low-pass filtering leads to errors in bridges with a low first natural frequency. In these bridges, filtering can inadvertently remove a significant part of the static response. In particular, it can be difficult to distinguish the effects of individual closely-spaced axles and filtering can lead to a reduction in the clarity of the individual effects.
- Compared to the problems mentioned before, a spectral Bridge WIM algorithm has the advantages: (a) No theoretical knowledge of the influence line is required; (b) Strain

measurements from each scan are not compared to corresponding theoretical values, but the contribution of each harmonic in frequency terms. This tends to reduce errors induced by inaccurate truck location (speed), (c) The frequency domain representation of the signal facilitates the suppression of high frequency effects and (d) The signal to work with is in a sense the 'true' one (No filtering or windowing effect that could have modified it, have been used).

However, the algorithm failed to accurately predict the weights of a lot of axles simultaneously. As a very good definition of low frequency components is not generally possible (due to the limited time the load is on the bridge), a high number of axles requires the use of equations for high frequency components of the signal. Higher frequency components generally have a smaller magnitude and their sensitivity to effects other than static response (i.e. dynamics) leads to unacceptable errors.

7.3 AN ALGORITHM BASED ON A BRIDGE DYNAMIC MODEL

The total strain response from a bridge due to a truck crossing can be modelled with a dynamic model based on constant loads. The total theoretical strain $\varepsilon(t)$ can be approximated as a function of the applied axle weights and the total (static + dynamic) strain response due to a unit moving load:

$$\varepsilon(t) = \sum_{i=1}^{no\_axles} W_i \varepsilon_{i1}(t) \tag{7.11}$$

where W_i is the axle weight corresponding to axle i, and $\varepsilon_{i1}(t)$ is the total strain due to a unit load moving at the vehicle speed and located at the position of axle i (Theoretical expressions for $\varepsilon_{i1}(t)$ are given in Section 5.3). The difference from Moses's approach would be the use of the dynamic response due to a unit load instead of the influence line. Variation in W_i is not taken into account.

The assumption of linearity and superposition involved in this formulation has been proven to match more realistic approaches (Dempsey & Brady 1999), even though the solution to the bridge-truck dynamic problem is non-linear. The theoretical model is also generated

with constant loads, so interaction between bridge and truck masses is neglected. This simplification allows a calculation in real time and a significant improvement in accuracy compared to the static algorithm based on the influence line. A more sophisticated model such as a quarter car could be considered instead of constant loads, but the difference in accuracy might not be justifiable due to the introduction of new unknown parameters.

The formulation for this dynamic B-WIM (DB-WIM) algorithm is derived by minimising an error function defined by the squared difference between measured and theoretical strains. The error function is:

$$\Psi = \sum_{t=1}^{no\_records} (\tilde{\varepsilon}(t) - \varepsilon(t))^2 \tag{7.12}$$

where $\tilde{\varepsilon}(t)$ is measured strain and $\varepsilon(t)$ is the total theoretical strain at a certain instant t given by 7.11.

By substituting Equation 7.11 into Equation 7.12, it is found that:

$$\Psi = \sum_{t=1}^{no\_records} (\tilde{\varepsilon}(t) - \sum_{i=1}^{no\_axles} W_i \varepsilon_{i1}(t))^2 \tag{7.13}$$

Ψ is minimised by differentiating and setting to zero.

$$\frac{\partial \Psi}{\partial W_i} = 0 \quad ; \quad i = 1, 2, \ldots, \text{no. axles} \tag{7.14}$$

which gives,

$$\sum_{t=1}^{no\_records} [\tilde{\varepsilon}(t) - \sum_{i=1}^{no\_axles} W_i \varepsilon_{i1}(t)] \varepsilon_{i1}(t) = 0 \quad ; \quad i = 1, 2, \ldots, \text{no. axles} \tag{7.15}$$

Re-arranging Equation 7.15 gives:

$$\sum_{t=1}^{no\_records} [\sum_{i=1}^{no\_axles} W_i \varepsilon_{i1}(t)]\varepsilon_{i1}(t) = \sum_{t=1}^{no\_records} \tilde{\varepsilon}(t)\varepsilon_{i1}(t) \tag{7.16}$$

or, in matrix form:

$$[T]\{W\} = \{H\} \tag{7.17}$$

where *[T]* is a matrix whose elements depend only on the total answer due to a unit load, axle spacings and speed,

$$[T_{ij}] = \sum_{t=1}^{no\_records} \varepsilon_{i1}(t)\varepsilon_{j1}(t) \tag{7.18}$$

{W} is a column vector composed of the unknown axle weights, and *{H}* is a column vector that depends on the measured strain as well as the total answer due to a unit load, axle spacing and speed.

$$\{H_i\} = \sum_{t=1}^{no\_records} \tilde{\varepsilon}(t)\varepsilon_{i1}(t) \tag{7.19}$$

Finally, axle weights are calculated as:

$$\{W\} = [T]^{-1}\{H\} \tag{7.20}$$

Gross Vehicle Weight (GVW) is obtained by summing the individual axle weights:

$$GVW = \sum_{i=1}^{no\_axles} W_i \tag{7.21}$$

Figure 7.7 illustrates the quality of the approximation obtained by DB-WIM to the simulated strains. The total strain and the static strain are obtained from numerical simulations (four degree of freedom model with mechanical characteristics described in Section 7.2.4). Another curve represents the strains obtained using Equation 7.11 if

considering constant loads. The DB-WIM system will be more accurate, the closer its adjustment is to the total strain.

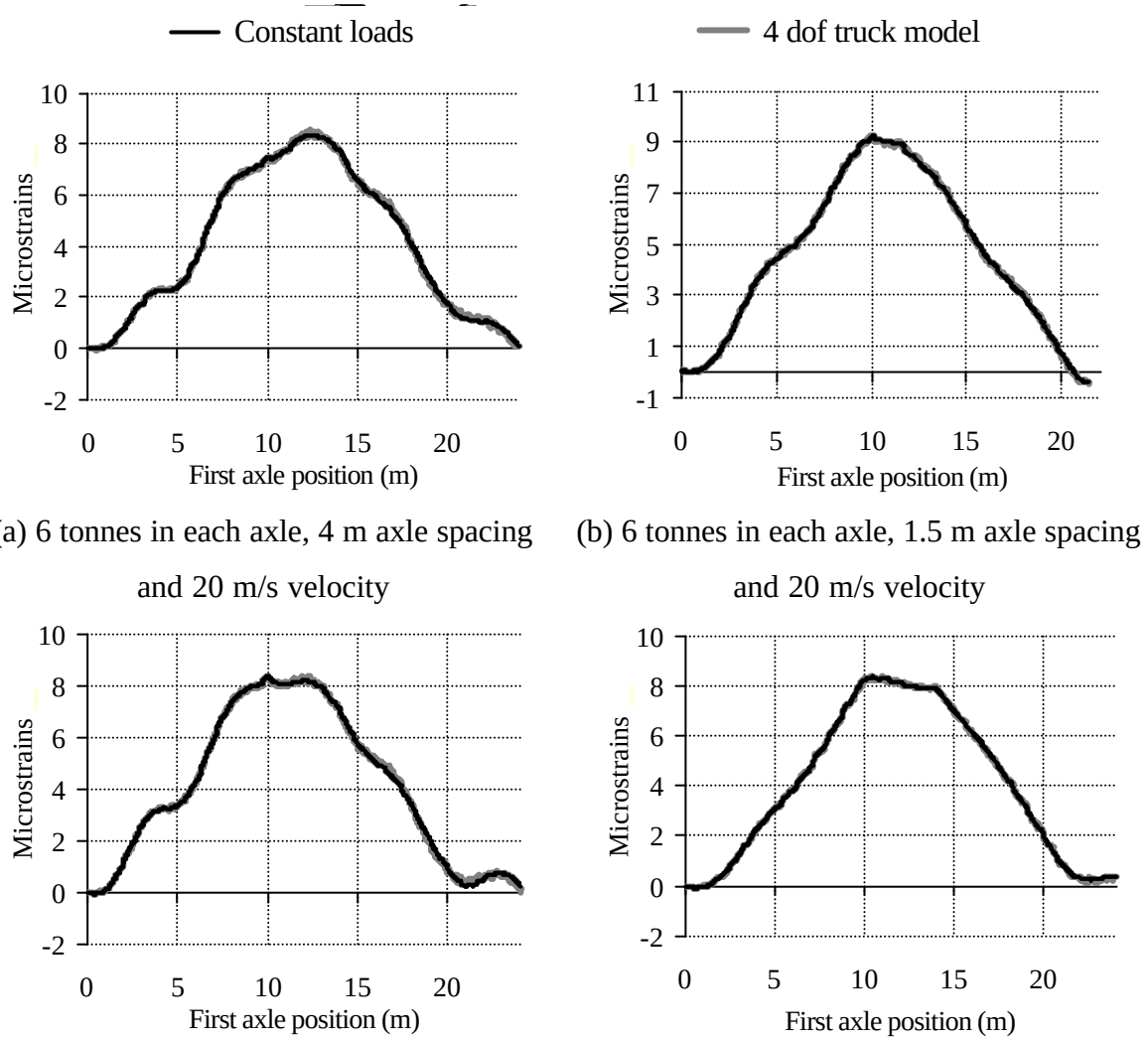

(a) 6 tonnes in each axle, 4 m axle spacing and 20 m/s velocity

(b) 6 tonnes in each axle, 1.5 m axle spacing and 20 m/s velocity

(c) 8.5 and 3.5 tonnes in each axle, 4 m axle spacing and 20 m/s velocity

(d) 6 tonnes in each axle, 4 m axle spacing and 30 m/s velocity

Figure 7.7 – Strain at midspan induced by a 2-axle vehicle and approximation by DB-WIM algorithm for different cases

Figure 7.8 shows the quality of the adjustment obtained by a static algorithm as proposed by Moses in comparison to the simulated static strain. In the case of Figure 7.8(d), it is possible to notice how the static approach overestimates the weight of both axles when trying to adjust the static answer to the total strain (the real static strain is unknown in measurements).

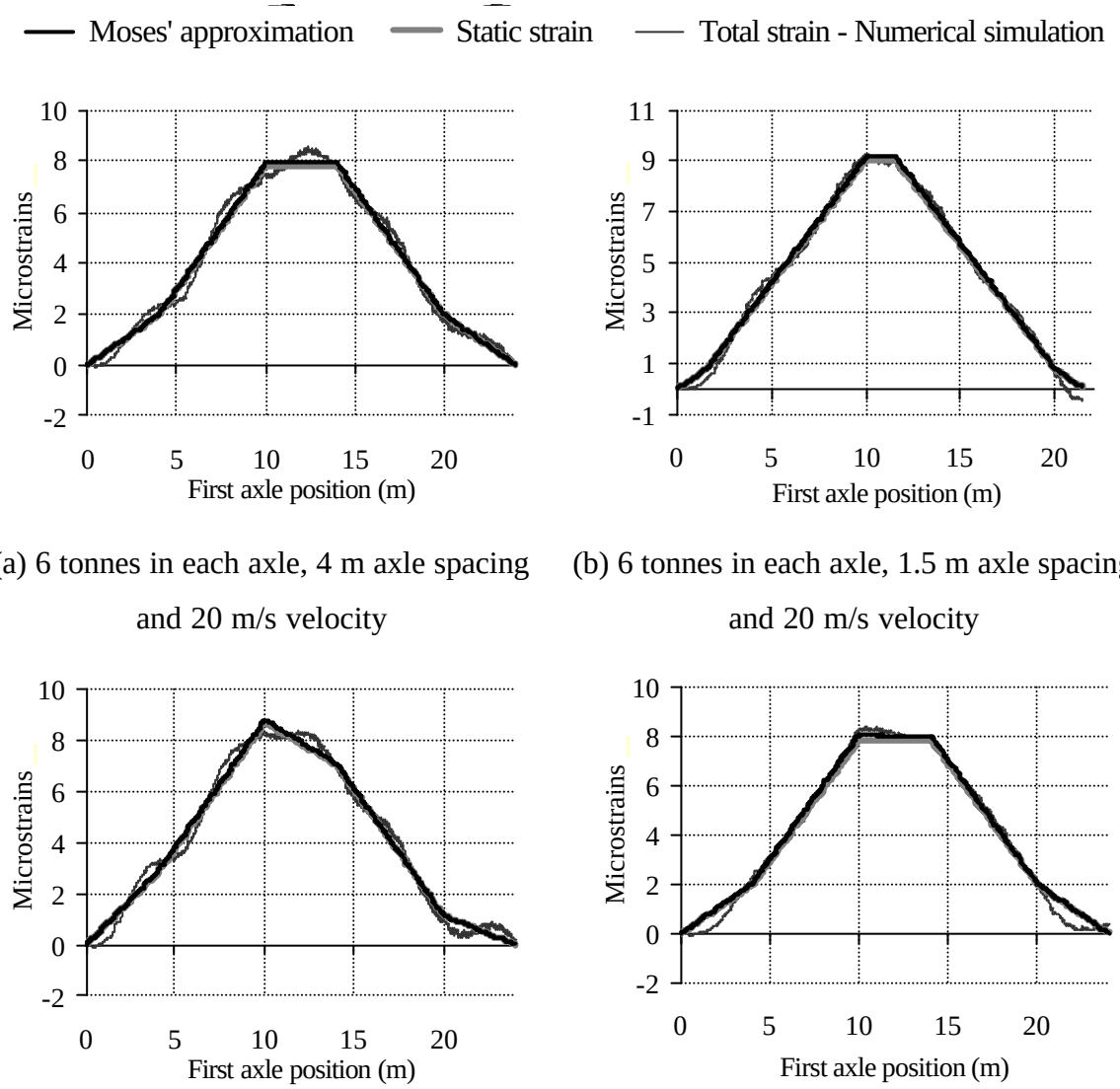

(a) 6 tonnes in each axle, 4 m axle spacing and 20 m/s velocity

(b) 6 tonnes in each axle, 1.5 m axle spacing and 20 m/s velocity

(c) 8.5 and 3.5 tonnes in each axle, 4 m axle spacing and 20 m/s velocity

(d) 6 tonnes in each axle, 4 m axle spacing and 30 m/s velocity

Figure 7.8 – Strain at midspan induced by a 2-axle vehicle and approximation by static algorithm for different cases

The results in Figures 7.7 and 7.8 correspond to a road profile in 'good' condition. In this case, the dynamic model based on constant loads achieves a solution very close to that obtained by a four degree of freedom vehicle model. Although a good road surface considerably increases the accuracy, other factors such as the presence of a bump at the expansion joint must also be taken into account. Some road classifications do not cater for this unevenness, which is responsible for high truck dynamic forces on the bridge (Section 3.5.1). The improvement of the dynamic algorithm over the static is especially important in the cases of frequency matching presented in the following subsection.

Influence of speed – frequency matching on B-WIM accuracy

When a load traverses a bridge, there is a pseudo-frequency associated with this passing given by:

$$frequency_{moving\_load} = Speed / Bridge\_Length \tag{7.22}$$

When this frequency is close to twice the natural frequency of the bridge, a static B-WIM algorithm could give significant errors in GVW due to the difference between the static and total strain. For a normal range of speeds and bridge dynamic behaviour (first natural frequency of the bridge decreasing as the bridge length increases), this frequency matching is more likely to happen in bridges over 30 m.

Figure 7.9 illustrates the influence on the accuracy of Moses' static algorithm when considering a two-axle vehicle at different speeds over a 40-m bridge (first natural frequencies: 1.06 and 4.26 Hz, strong damping 5%). The vehicle model is shown in Figure 7.3 (mechanical characteristics in Section 7.2.4). Solutions provided by Moses for simulations at three vehicle speeds 20, 25 and 30 m/s (equivalent to frequencies 0.5, 0.625 and 0.75 Hz respectively) are represented. The bridge response does not have a sufficient number of dynamic oscillations and Moses' adjustment differs from the simulated static strain (which should be symmetric in Figures 7.9(a) and (c)). Error in axle weights is significant.

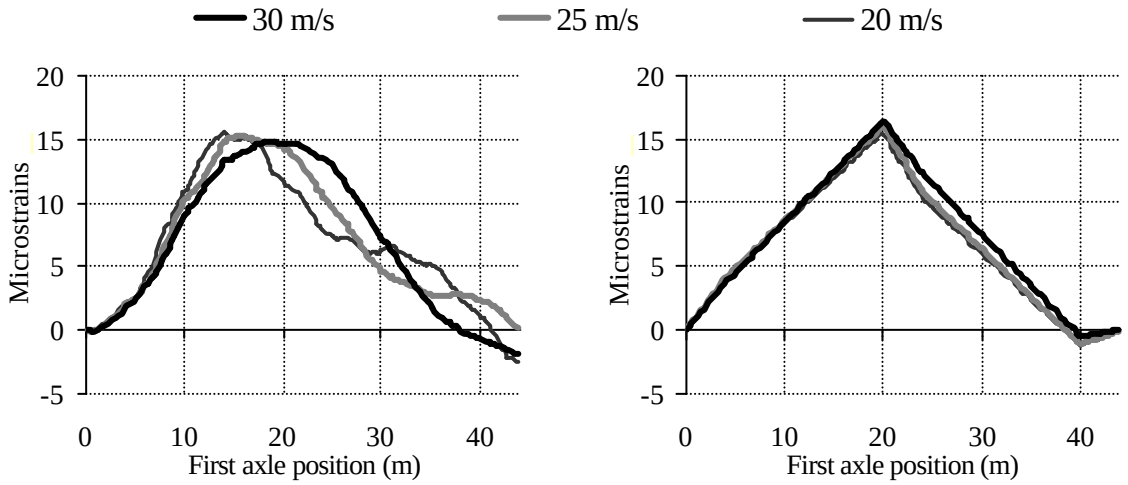

(a) Total strain due to weights: 6 + 6 t (b) Moses's solution to (a)

Figure 7.9 (continued on following page)

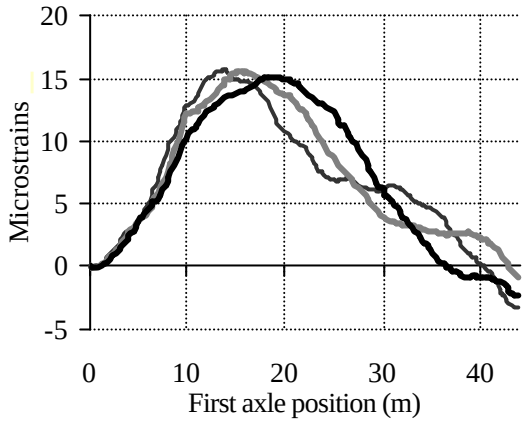

(c) Total strain due to weights: 8.5 + 3.5 t

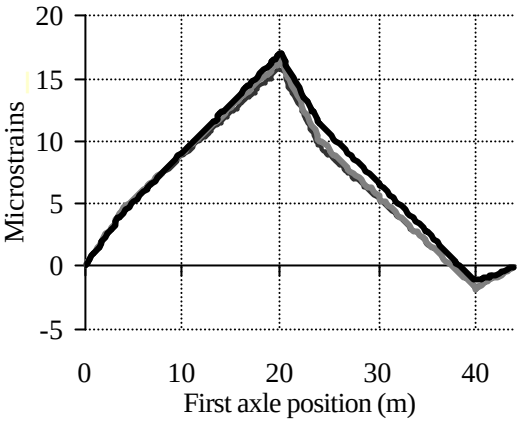

(d) Moses's solution to (c)

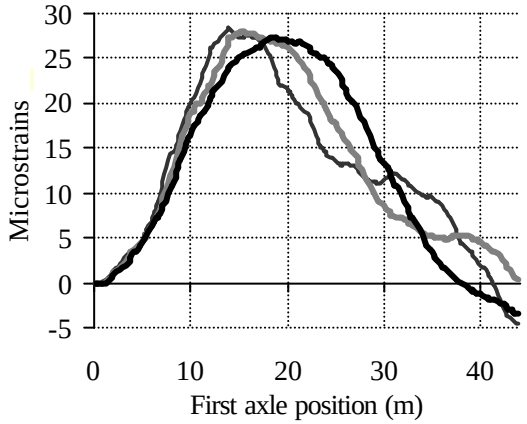

(e) Total strain due to weights: 11 + 11 t

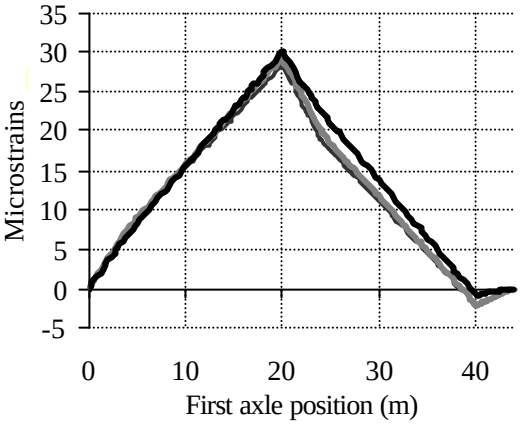

(f) Moses's solution to (e)

Figure 7.9 – Static adjustment for different axle weights in a 40-m bridge

Figure 7.10 shows the ideal calibration factor for this bridge at different vehicle speeds. This static calibration factor was obtained dividing the real GVW by the estimated GVW. The calibration factor is the same for the two vehicles of weight equally distributed between axles (6+6 and 11+11), but changes when the axle weight distribution is different. There is a tendency to overweigh vehicles as the speed increases.

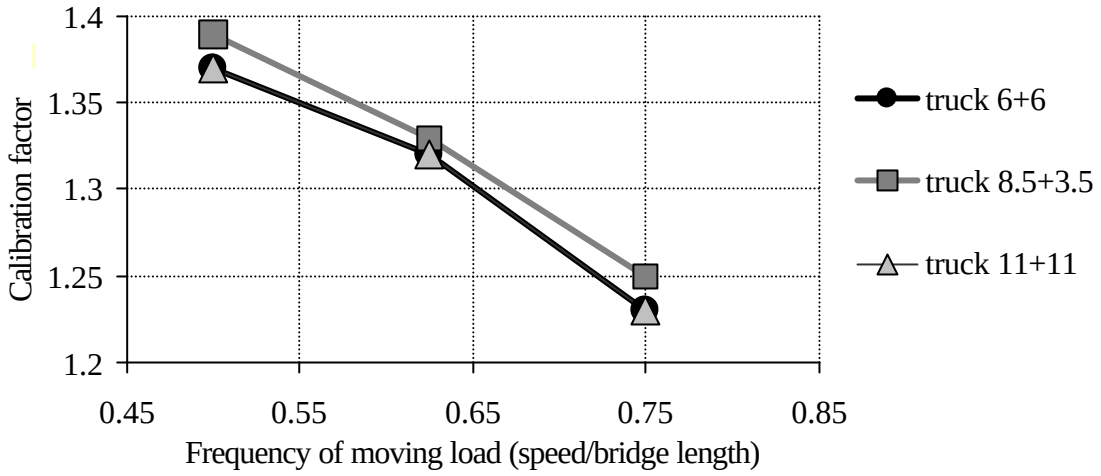

Figure 7.10 - Calibration factors obtained for the 40-m bridge

The dynamic approach gave the following results:

- The preceding cases with a small number of oscillation periods are solved satisfactorily.
- Truck dynamics are removed through a least square fitting of all the readings along the bridge. The value that is obtained for static weight should be very close to the correct value.
- Bridge mass/inertia is taken into account in the formulation. No filtering techniques that rely on a sufficient number of vibration periods for a safe removal of bridge dynamics are necessary.

As a conclusion, a DB-WIM algorithm looks to be a more satisfactory solution that caters accurately for more bridge and truck types than traditional static B-WIM algorithms. It caters better for those cases with a low first natural frequency that could not be smoothed properly by static B-WIM, or records where vehicles travel at high speed, and in general, situations where the induced dynamic effects are large. A good solution can be identified in the field when the theoretical strain generated by the bridge dynamic model of DB-WIM matches the measured strain. This algorithm is based on one longitudinal sensor location, though it will be further extended to multiple sensors in Section 7.5.1. The performance of DB-WIM will be tested in Chapter 9.

7.4 AN ALGORITHM BASED ON A TRUCK DYNAMIC MODEL

The non-linear approach described in this section is based on the application of optimisation techniques to allow for the dynamic modelling introduced in Chapter 5. The bridge-car structural system has an infinite number of degrees of freedom and only a limited number of them given by the strain readings are available (apart from strains, some dynamic characteristics of the bridge such as first natural frequencies and damping can be obtained experimentally). The first limitation is the fact that it is strains that are measured, as dynamic equations are related to displacements, velocities and accelerations of the deformed shape. To convert strains into displacements or vice versa, it is necessary to make assumptions on the bridge dynamic behaviour.

7.4.1 Optimisation Process

The objective function is given by the sum of squared differences between the measured and theoretical strains for each record in time. The optimisation process is summarised in Figure 7.11. The iteration process requires:

- Initial conditions given by a static B-WIM system. These initial conditions (i.e. speed, axle spacing, axle weights) play a very important role in the achievement of the correct solution,
- Optimising results given by the dynamic simulation of the truck on the bridge. In every case, the bridge is modelled as described in Section 5.2. The equation of motion corresponding to the bridge is:

$$EI\frac{\partial^4 z(x,t)}{\partial x^4}+m\frac{\partial^2 z(x,t)}{\partial t^2}+2m\omega_b\frac{\partial z(x,t)}{\partial t}=\sum_{i=1}^{n}\varepsilon_i\delta(x-x_i)R_i(t) \qquad (7.23)$$

where :

$z(x,t)$: displacement of the bridge at position x and time t,

E, m and I : Young's modulus, mass per unit length, and second moment of area of the bridge respectively,

δ : Dirac function,

ε_i = 1 when axle i is on the bridge (otherwise zero),

w_b = xw_n is damping frequency, where x is damping and w_n is natural frequency of the bridge,

n : number of axles,

$R_i(t)$: the interaction force between the bridge and the applied axle load i,

x_i = $vt - a_i$, is the position of axle i (the position of first axle is $x_1 = vt$), where a_i is spacing between first axle and axle i, and v is velocity.

- Truck modelling that can have different parameters: (a) Consider axles as constant loads, (b) Consider axles as masses or (c) Consider axles as sprung masses. The introduction of truck models based on more degrees of freedom does not result in a more accurate solution necessarily as new parameters can lead to an iterative process that does not converge.

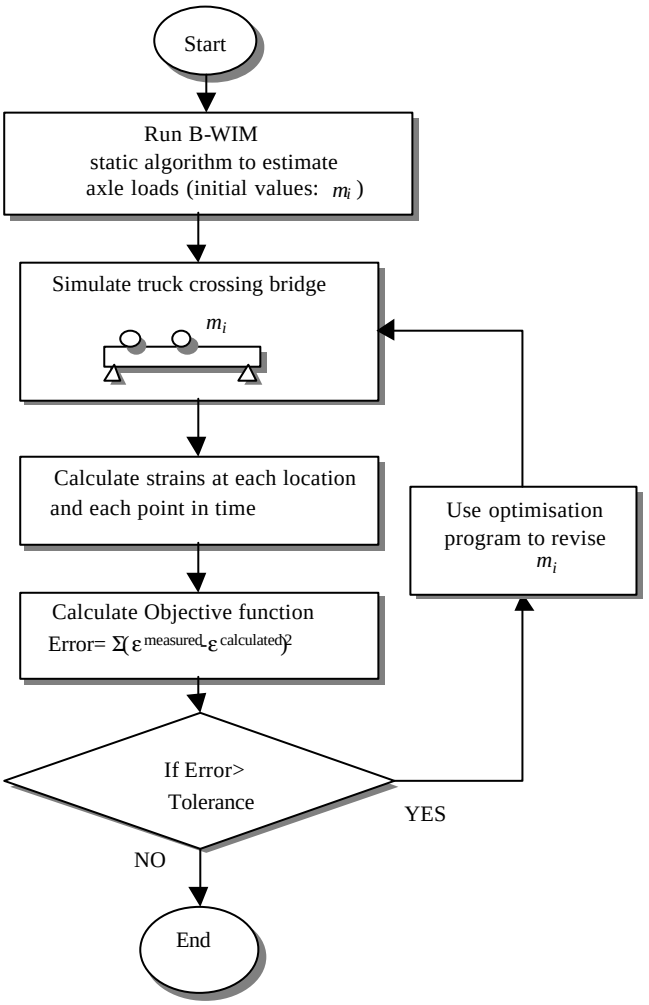

Figure 7.11 – Optimisation process

(a) Consider axle loads as constant loads

Axle loads are assumed to be constant and equal to the static weights. This assumption can be acceptable in long span bridges where the vehicle mass is negligible compared to the bridge mass. Parameters to optimise: R_i, axle force.

When vehicle axles are modelled as constant loads, speed (v), axle spacing (a_i) and loads ($m_i g$) for each axle define the vehicle parameters to be optimised. Equations 7.24 represent the applied forces in this simplified model.

$$m_i g = R_i \qquad ; \quad i = 1,2,...n \tag{7.24}$$

where n is number of axles.

(b) Consider axle loads as moving masses

Inertial effects of the axle mass are taken into account. It is assumed there is no redistribution of load between axles. Compared to the dynamic model based on constant loads, this modelling can improve accuracy in short span bridges.

Speed (v), axle spacing (a_i) and masses (m_i) for each axle define the parameters to be optimised. Mass is optimised until the difference between one value and the next one is sufficiently small. The iteration will stop when the difference between the value of the parameters for an iteration and the preceding one is within a given threshold.

The moving mass has one degree of freedom that represents vertical displacement. Equations 7.25 represent the vertical motion (z_i) of the moving masses (m_i),

$$m_i g - \frac{m_i d^2 z_i(t)}{dt^2} = R_i(t) \qquad i = 1,2,...n \tag{7.25}$$

where n is number of axles. The systems of differential Equations 7.23 and 7.25 can be solved with the method of Runge-Kutta (Appendix E).

(c) Consider axle loads as moving masses with stiffness elements (sprung masses)

The mass and stiffness of the axle force are taken into account in the axle modelling. An instantaneous interaction force R_i can be obtained at each instant by optimising strain at a number of sensors. The objective function for this process is given by the sum of the squared differences between measured strain and theoretical strain for each sensor. This interaction force takes account of the road irregularities. A second iterative process (Figure 7.10) optimises speed (v), and masses (m_i) and axle spacings (a_i) for each axle.

Each moving mass is allowed to move in the vertical direction. Equations 7.26 represent the vertical motion (z_i) of the moving masses (m_i),

$$m_i g - \frac{m_i d^2 z_i(t)}{dt^2} - R_i(z_i, t) = 0 \qquad i = 1,2,...n \tag{7.26}$$

where n is number of axles.

Equation 7.27 represents the interaction force $R_i(z_i,t)$ between the bridge and the wheel at the contact point.

$$R_i(z_i, t) = K_i[z(x_i, t) - r(x_i)] \tag{7.27}$$

where $r(x_i)$ is the road profile.

The Runge-Kutta method can be used to solve Equations 7.23, 7.26 and 7.27. If the masses m_i are known (i.e. calibration vehicle), interaction forces can be calculated accurately at each instant. This information can be useful to analyse dynamic wheel forces.

While truck models (a) and (b) assume a smooth road profile, approach (c) tries to take account of the road irregularities by allowing for an assumed tyre stiffness at each instant. This optimisation at each instant is only feasible if there are a sufficient number of sensors.

7.4.2 Objective Function

The objective function for the numerical simulation of a 12 tonne two-axle rigid body running over a 20-m bridge (4.26 Hz first natural frequency) is analysed for both the static and dynamic algorithms based on constant loads. The characteristics of the truck are given in section 7.2.4. The results of the simulation and adjustment based on bridge dynamic model are shown in Figure 7.12.

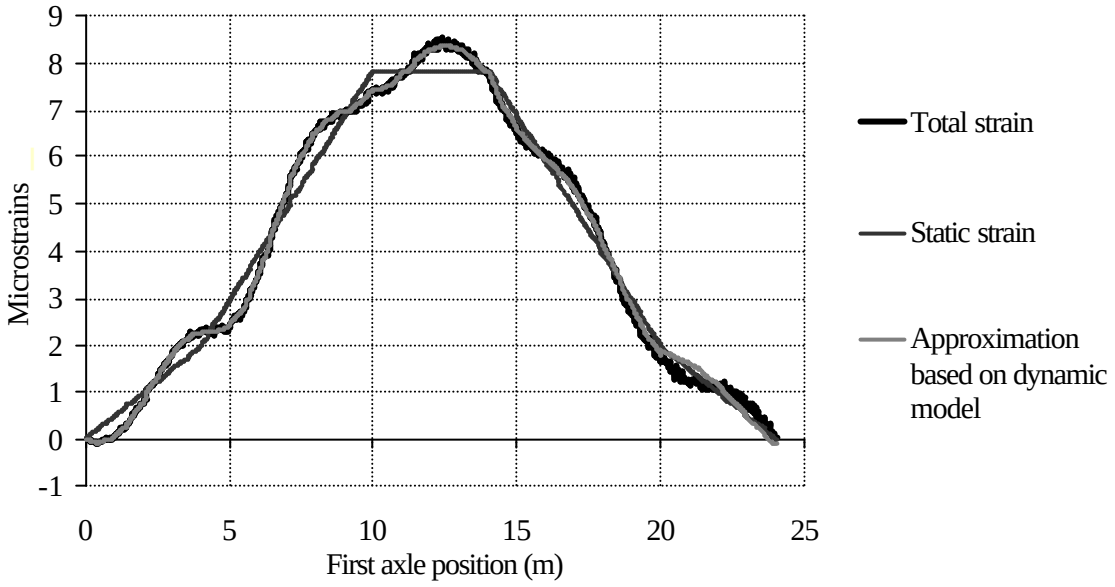

Figure 7.12 – Simulation of a two-axle rigid body

Axle weights are obtained using the static and dynamic algorithms. All variables are fixed, except front and rear axle weight. The contours of the objective function for front and rear axle weight are represented in Figure 7.13. The objective function has a minimum. For the dynamic approach, the solution fits in the centre of the central area in Figure 7.13(f). For the static approach, the solution is not perfectly symmetric, and the rear axle tends to be overweighed due to dynamics. Appendix G illustrates the values of the objective function for other combinations of parameters (speed, axle spacing and axle weights).

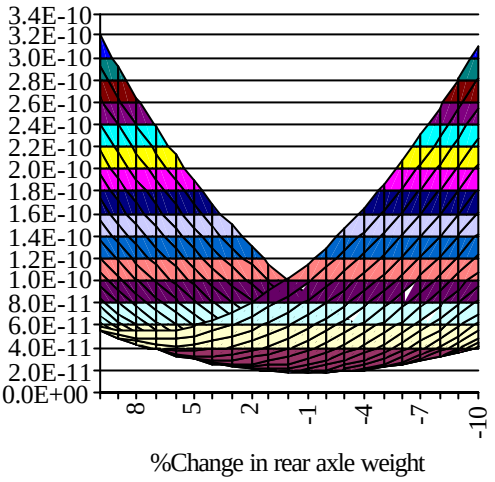

(a) Linear static approach (-10% to 10%)

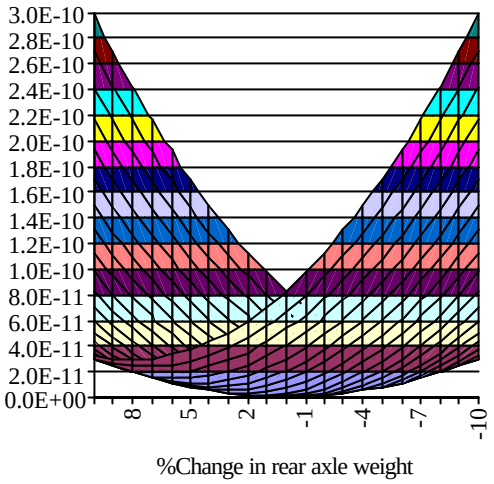

(b) Linear dynamic approach (-10% to 10%)

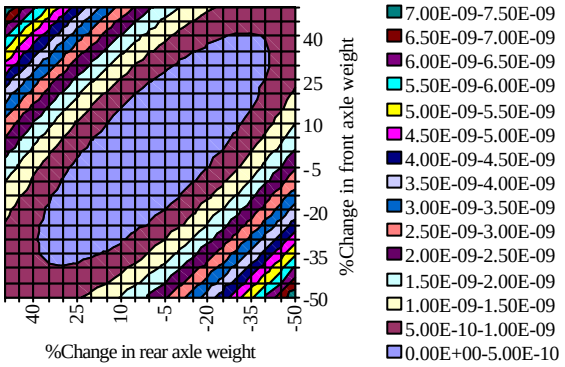

(c) Linear static approach (-50% to 50%)

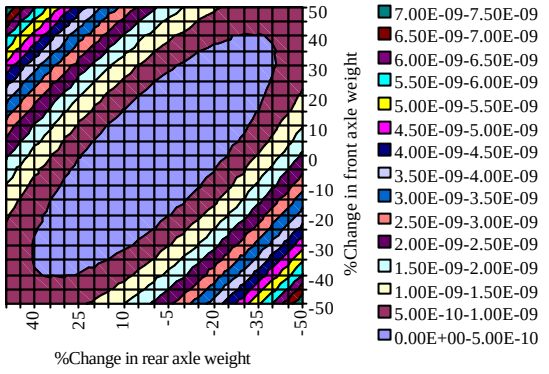

(d) Linear dynamic approach (-50% to 50%)

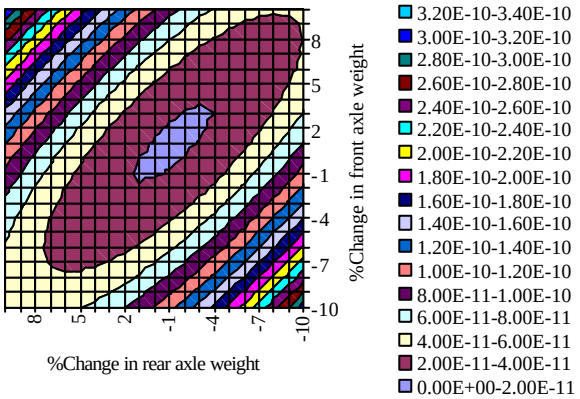

(e) Linear static approach (-10% to 10%)

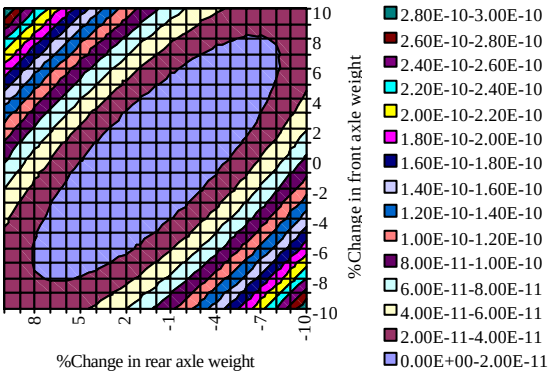

(f) Linear dynamic approach (-10% to 10%)

Figure 7.13 – Objective function for variables: Front and Rear axle weight

A vehicle of the same mechanical characteristics but different redistribution of weight between axles (8.5 tonnes in the front and 3.5 in the rear axle) is also used to test the objective function. The dynamic algorithm based on constant loads was used to generate

the theoretical strain. Figure 7.14 represents this function when allowing axle weight to change while fixing the rest of the parameters.

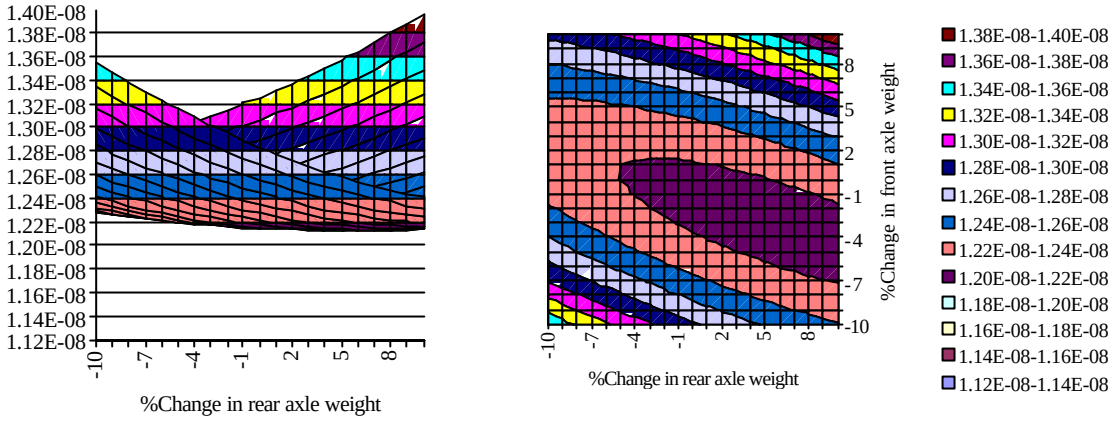

(a) SideView (-10% to 10%) (b) PlanView (-10% to 10%)

Figure 7.14 – Objective Function for different weight distribution (Dynamic algorithm)

The same dynamic algorithm (based on constant loads) is applied to nine different locations simultaneously (simulated strain at all locations is added together). The objective function is defined as the sum of the differences between predicted and simulated strain at every location. Figure 7.15 shows the values of the objective function (variables: front and rear axle weights) if using the sum of nine sensors equally distributed along the bridge instead of one sensor at midspan (Figure 7.14). In this case, there is not significant improvement in the estimation of static weights by increasing the number of sensors.

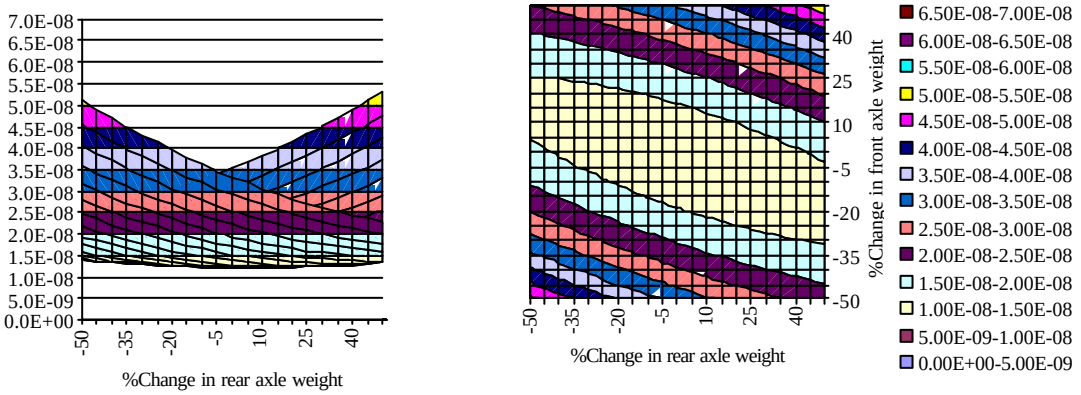

(a) SideView (-50% to 50%) (b) PlanView (-50% to 50%)

Figure 7.15 – Objective Function for different number of sensors

7.5 ONE-DIMENSIONAL MULTIPLE-SENSOR ALGORITHMS

The multiple-sensor static algorithm introduced in Section 3.5.4 (Kealy & O'Brien 1998) tries to find the applied force applied along the bridge using multiple longitudinal sensor locations. This results in a number of strain records for each point in time, permitting the possibility of instantaneous axle and gross vehicle weight calculation. An equation based on the influence line for each location can be formulated for each sensor at each instant. However, the static approach has limitations resulting from the dependency of the equations. The system can be solved for a fixed number of axles related to the degree of indeterminacy of the structure: 2 axles in a single span, 3 in a continuous two span-bridge, etc… The algorithm introduced in this section overcomes this limitation by using a high number of sensors and applying a least square fitting technique. The dynamic response can also be adopted as a reference in a multiple-sensor algorithm. In another words, the measured strain is compared to the theoretical total strain instead of the static strain (given by influence lines).

7.5.1 Dynamic Multiple-sensor Algorithm

A dynamic algorithm capable of calculating instantaneous values of axle force as the truck travels across the bridge is introduced. This algorithm is based on measurements at multiple sensor locations in the longitudinal direction. The axle load at each instant can be calculated from the theoretical dynamic strain response at these locations due to a single load. The static value is given by the root mean square of axle forces from the force history. The advantages of this new approach is that bridge dynamics are removed from the experimental strain record without the need for filtering that could remove some significant static component. Additional information will stem from knowing the complete history of dynamic axle forces applied to the bridge: dynamic amplification factors, data for fatigues studies and spatial repeatability and collection of truck dynamic characteristics through spectrum analysis of the applied load.

Formulation

This multiple-sensor system is based on the accurate determination of the theoretical strain response due to a moving constant load at different bridge locations. This is obtained by a) experimental determination of the natural frequencies and damping of the bridge, b)

calculation of the mode shapes based on the bridge geometry, and c) adjustment of the unit response curves to give a best fit to the known loads applied by the calibration vehicle. Each sensor location is calibrated differently. The axle weights are considered to be moving loads, and the effect of their mass is neglected compared to the mass of the bridge. This approach assumes linearity and the principle of superposition when several loads are applied to the bridge at the same time.

The total strain response ε_k from a bridge due to a truck crossing can be modelled with a dynamic model based on constant loads. The total theoretical strain $\tilde{\varepsilon}_k(t)$ at a certain location *k* can be approximated as a function of the applied axle weights W_i and the total (static + dynamic) strain response due to a unit moving load, $\varepsilon_{ki}(t)$ (Section 5.3) as follows:

$$\tilde{\varepsilon}_k(t) = \sum_{i=1}^{n} \varepsilon_{ki}(t) W_i \tag{7.28}$$

where *n* is the number of axles. In matrix form,

$$\{\tilde{\varepsilon}\}_{kx1} = [\varepsilon]_{kxn} \{W\}_{nx1} \tag{7.29}$$

If there are a number of sensors, *k*, equal to the number of axles *n*, it is possible to formulate the following system of equations at each instant, *t*:

$$\{W\}_{nx1} = [\varepsilon]_{nxn}^{-1} * \{\tilde{\varepsilon}\}_{nx1} \tag{7.30}$$

where:

$\{\tilde{\varepsilon}\}_i$: measured strain due to the total applied load at longitudinal location *i*,

$[\varepsilon]_{ij}$: theoretical strain at sensor location *i* due to a unit moving load located at *j*,

$\{W\}_j$: applied load at location *j*,

n : total number of axles on the bridge.

The system of equations 7.30 is limited by the vehicle length and weight, which is assumed to be negligible compared to the corresponding length and weight of the bridge (long span bridges). It is therefore invalid for shorter bridges. However, the simulations described in this section would suggest that it gives results that are useful, being more accurate than existing static methods. On this basis, the method is being investigated further, despite the fact that it is theoretically unproven at this time.

There are certain critical locations: i.e., at the start and end of the bridge where small strains introduce rounding errors (these locations should not be considered in the calculations). If the determinant of the influence line matrix, $|e|$ is null for a combination of sensors, it is necessary to choose a different location. The value of this determinant will be analysed in Section 7.3.2.

The spectrum of the calculated axle loads $\{W\}$ can be obtained. The static value is the component of zero frequency of this spectrum. In practice, the static value is obtained through the root mean square of all instantaneous axle values.

Theoretical testing

Theoretical bridge-truck interaction models are used to generate strains at different locations along the bridge that allow the feasibility of the multiple-sensor system to be studied. Road surface irregularities are idealised as a stochastic process and generated from power spectral density functions as suggested by the International Standards Organisation. The bridge modelled is a simply supported 20 m single span with a first natural frequency of 4.26 Hz and 1% damping. Bending strains are obtained numerically at 9 different locations equally spaced along the bridge length. A 2-axle vehicle is modelled numerically (Figure 7.3) to analyse the influence of truck parameters during calibration. The data for the vehicle is given in Section 7.2.4. The performance of the dynamic multiple-sensor Bridge WIM algorithm is compared to a static approach (Moses 1979) for each simulation.

Figure 7.16 shows the information on strains required for the application of the algorithm. Referring to Equation 7.30, Figures 7.16(a), (c) and (e) give the components of the influence line matrix $[e]$ for each sensor and load position. Figures 7.16(b), (d) and (f)

present the variation in the components of $\{\tilde{e}\}$, the simulated strains at different fixed points, with distance travelled by the moving load.

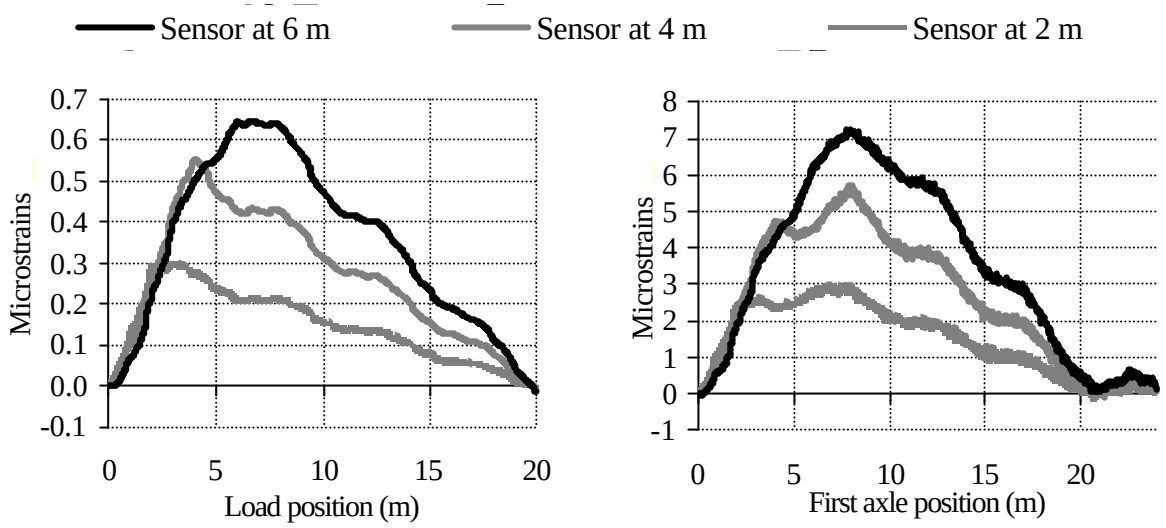

(a) Total strain due to a moving unit load at sensor locations: 2, 4 and 6 m

(b) Total strain due to a 2-moving axle body at sensor locations: 2, 4 and 6 m

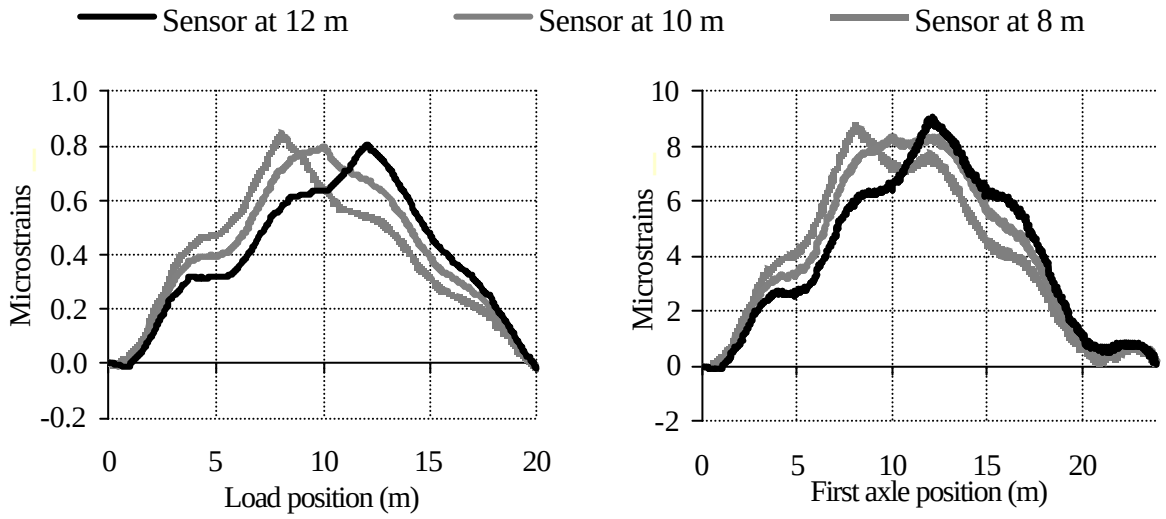

(c) Total strain due to a moving unit load at sensor locations: 8, 10 and 12 m

(d) Total strain due to a 2-moving axle body at sensor locations: 8, 10 and 12 m

Figure 7.16 (continued on following page)

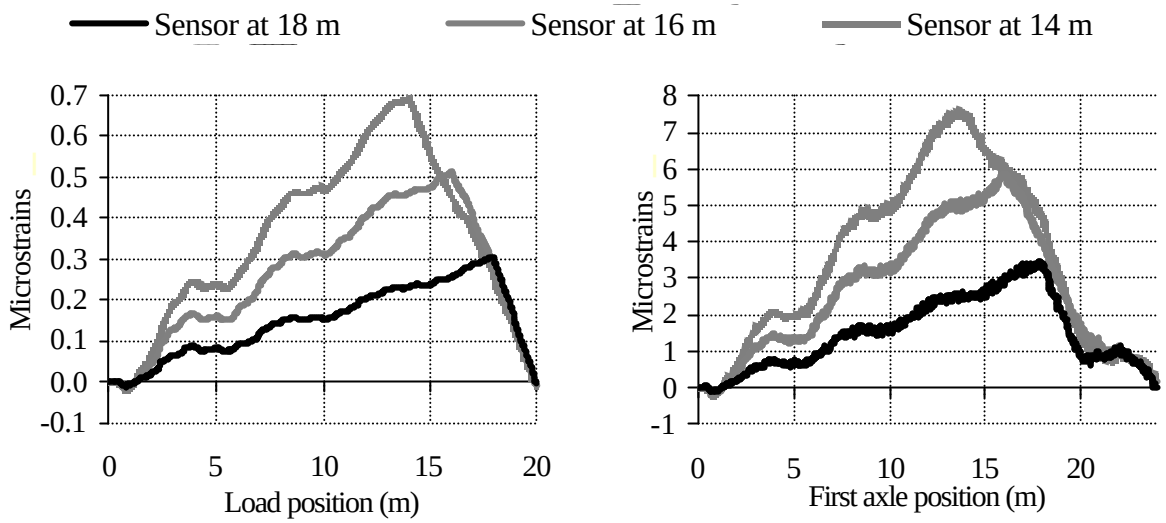

(e) Total strain due to a moving unit load at sensor locations: 14, 16 and 18 m

(f) Total strain due to a 2-moving axle body at sensor locations: 14, 16 and 18 m

Figure 7.16 – Total strain in different sensor locations

Figure 7.17(a) presents the variation of a calculated axle load, one component of *{W}*, with distance along 2 meters of the bridge. The corresponding applied axle load used for the simulation is included for comparison. Figure 7.17(b) is the spectrum of the predicted load variation for the first axle. From this spectrum an accurate static value of 6 tonnes can be obtained, in excellent agreement with the actual weight. A root mean square of all instantaneous axle values is generally preferred to obtain the static value.

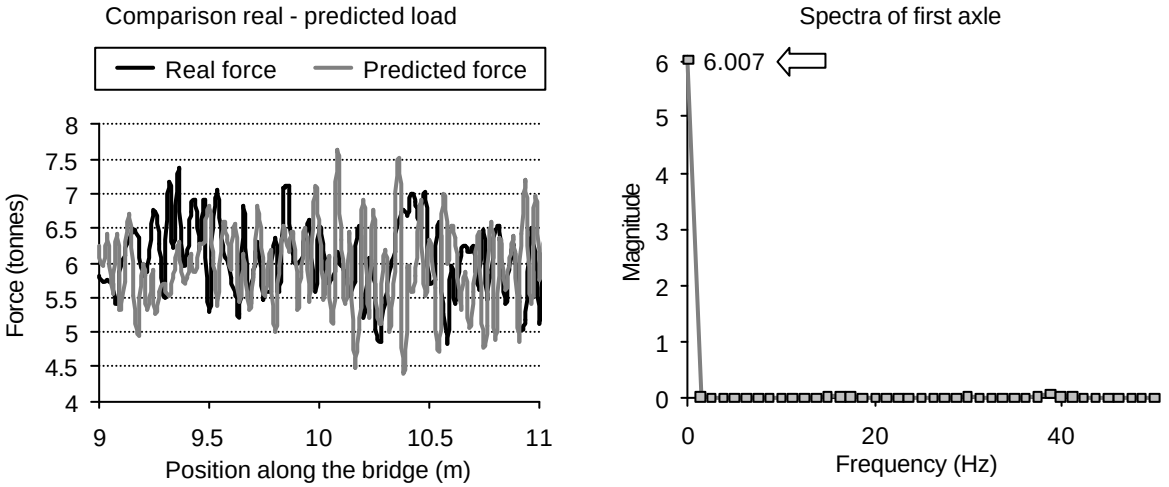

(c) Determination of instantaneous force

(d) Spectra of axle load history

Figure 7.17 – Short-term calculation

The accuracy of BWIM algorithms is sensitive to changes in some truck mechanical characteristics as compared to those used during calibration. The effect of altering certain vehicle parameters on the dynamic algorithm is studied by modifying its value by a percentage while leaving the rest of the parameters unaltered. Some of these parameters are a distribution of load between axles, axle spacing and tyre stiffness. The gross vehicle weight is the same in each case. The performance of the dynamic multiple-sensor Bridge WIM algorithm is compared to a static approach (Moses 1979). Figures 7.18(a) and (b) give the maximum relative error in weights for both the static and the new algorithms due to differences in the axle spacing and the position of the centroid of the body mass. Both algorithms are very accurate when there is only a change in axle spacing of the calibration truck. While the static algorithm gets more inaccurate when both axles are very closely spaced (tandem configurations), the new algorithm achieves the same degree of accuracy. When the body weight distribution between the axles changes, the dynamic algorithm is generally more accurate and shows a smaller standard deviation.

In the same way, the influence on accuracy of a difference in tyre stiffness is illustrated in Figure 7.18(c). A significant error appears for a decrease of 25% in the tyre stiffness as a result of a lower axle hop frequency. This very low frequency yields an average value far from the static weight. Figure 7.18(d) represents the applied load against axle position for this case. The inaccuracy is a consequence of the reduced number of available cycles of strain readings due to bridge length and speed. This limitation prevents the removal of that low frequency component in the spectrum. However, the 0.2 Hz frequency of this example is only a theoretical case, not a realistic one. In practice, these truck frequencies will be around 2 Hz, which correspond to an increase of the tyre stiffness in the graph. For these cases, the performance of both algorithms is good. The results show an improvement in the estimation of axle weights and a significantly smaller standard deviation when applying the multiple-sensor algorithm.

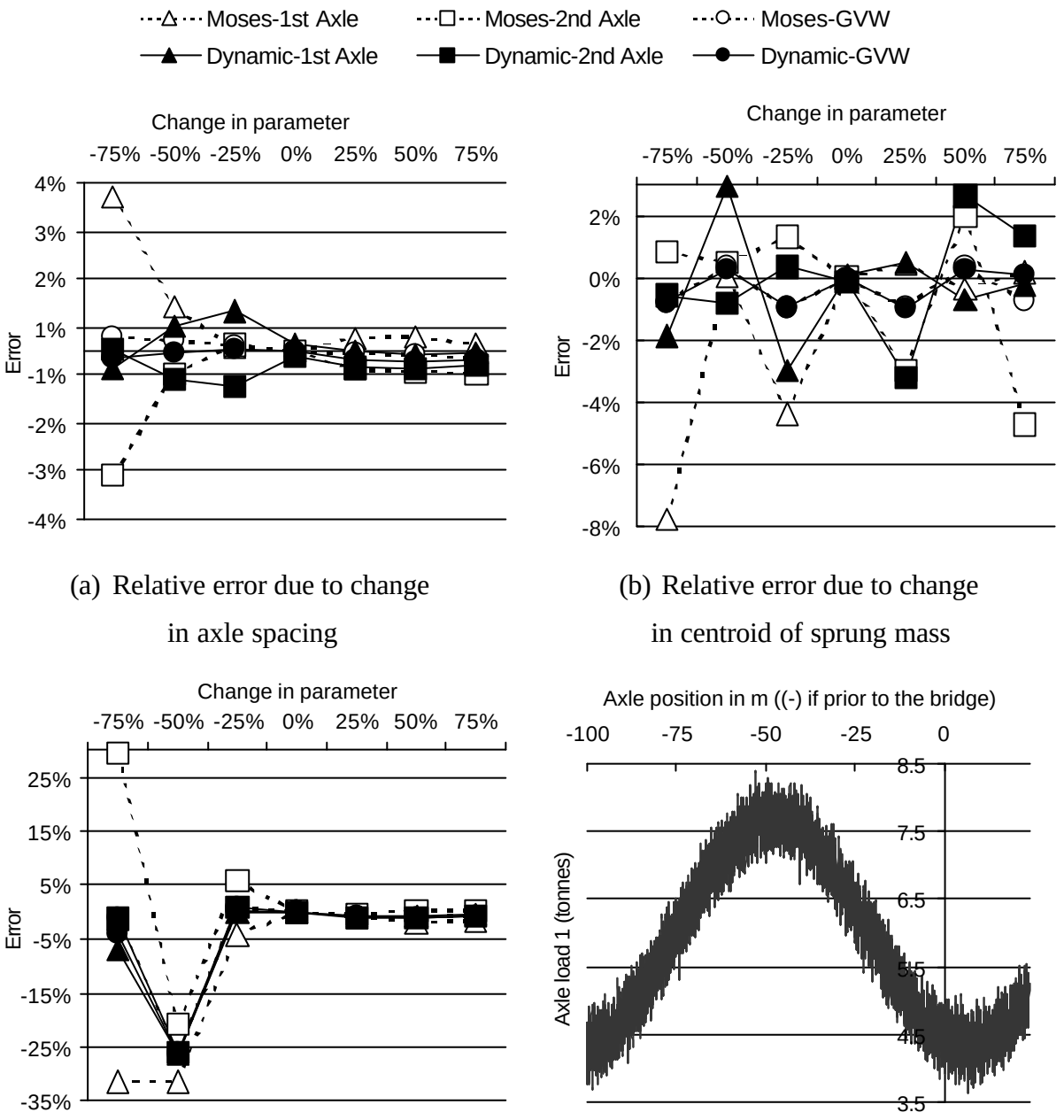

(a) Relative error due to change in axle spacing

(b) Relative error due to change in centroid of sprung mass

(c) Relative error due to change in tyre stiffness

(d) Applied load in the case of a decrement of 25% in tyre stiffness

Figure 7.18 – Effect on accuracy of the change of vehicle mechanics

Advantages and Disadvantages

The new algorithm achieves a considerable reduction in errors for individual axle weights. It is also less sensitive to truck mechanical characteristics than the traditional static approach. The traditional static algorithm is still very competitive for GVW. Some improvements introduced by the new approach are:

- There is always an error in the evaluation of a static axle load derived from the limitation in the definition of the applied load with time (Small samples are too sensitive to road profile, truck mechanics, etc.). This problem is significantly reduced with bridges where load can be defined for most of the bridge length based on the new approach introduced herein. Low speeds benefit this calculation. From spectral analysis of the varying axle loads, other frequency components can also be studied and mechanical characteristics of the truck collected depending on the road surface.
- No filtering of the strain signal is required. Bridge dynamics are removed during application of the dynamic equations of the algorithm. After applying the algorithm, the behaviour of the truck loads remains. Hence, the danger is removed of suppressing a significant static component through filtering over a relatively low first natural frequency of the bridge, especially if the vehicle speed is high and/or the axle spacings are small.

7.5.2 A Least Squares Fitting Multiple-sensor Algorithm

This section presents a further development on the approach initiated by Kealy & O'Brien. The algorithm formulates a system of static equations at each instant. Each of these equations is based on the influence line for each sensor location at each instant. However, this static approach has limitations due to the dependency of the equations, which relate applied load to measured strain. The equations can be solved for a limited number of axles related to the degree of indeterminacy of the structure: 2 axles in a single span, 3 in a continuous 2-span bridge, etc. The procedure that follows overcomes the limitations of the original approach by using a lot of sensors and applying an optimisation technique. The same technique can be applied to the dynamic multiple-sensor algorithm from the previous section.

The coefficients of the matrix $[e]$ in Equation 7.30 can be calculated taking as reference the total answer due to a single load (dynamic multiple-sensor B-WIM) or the influence lines (static multiple-sensor B-WIM). If the determinant $|e|$ is null, there will not be solution. The influence lines corresponding to the example in Figure 7.16 are represented in Figures 7.19(a), (c) and (e). The static strain depends directly on the applied load, its location on the bridge, the Young's modulus and section modulus at the sensor location. This static strain is directly proportional to the applied load. The differences between the

theoretical static and dynamic strain due to a unit moving load are shown in Figures 7.19(b), (d) and (f). As expected, the dynamic deviation is higher for the locations near midspan. This dynamic strain corresponds to a moving load travelling at 20 m/s. Unlike the static component, the total strain for a given load depends on its speed, so there is a different reference for each speed.

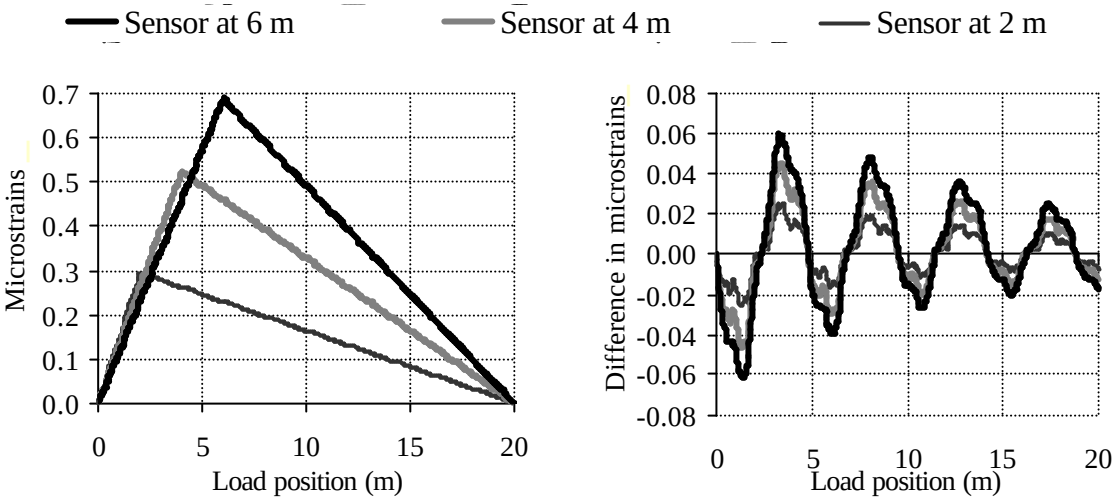

(a) Influence lines at 2, 4 and 6 m

(b) Difference between dynamic answer due to a unit load and influence lines of (a)

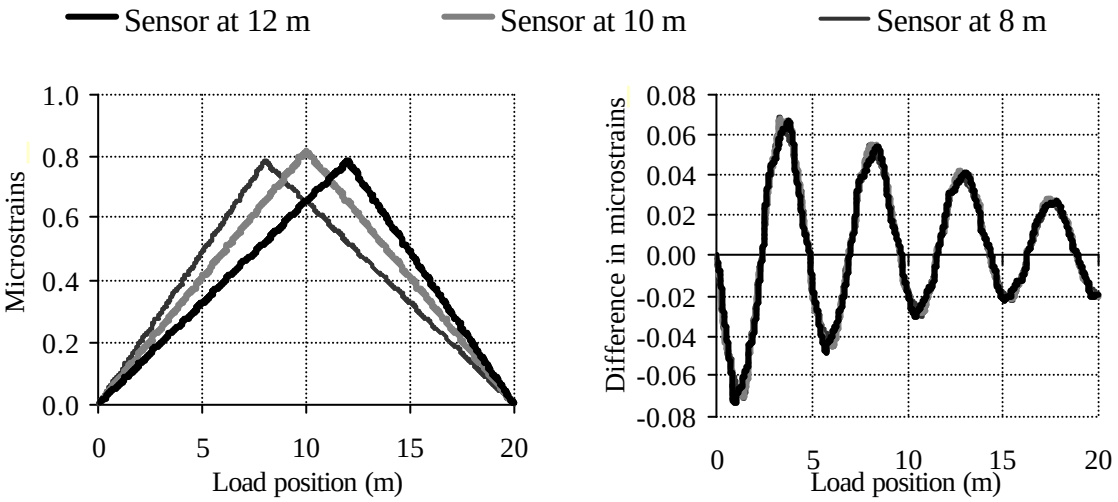

(c) Influence lines at 8, 10 and 12 m

(d) Difference between dynamic answer due to a unit load and influence lines of (c)

Figure 7.19 (continued on following page)

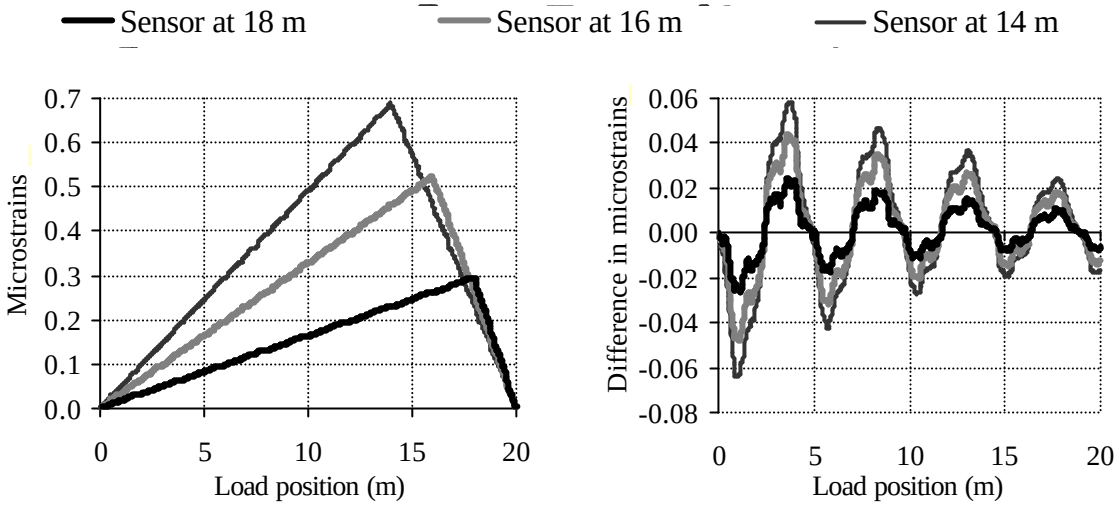

(e) Influence lines at 14, 16 and 18 m

(f) Difference between dynamic answer due to a unit load and influence lines of (e)

Figure 7.19 – Static response for 9 different locations equally spaced along the bridge

The value of the determinant obtained by applying the static and dynamic multiple-sensor B-WIM systems are compared in Figure 7.20. The static and total responses due to a unit load represented in Figures 7.19 and 7.16 respectively are used to generate the determinant for different combination of sensors. The values of the determinant are given since the first axle is at 4 m from the bridge support. This is the vehicle axle spacing and the position where simultaneous calculation of the two axles start.

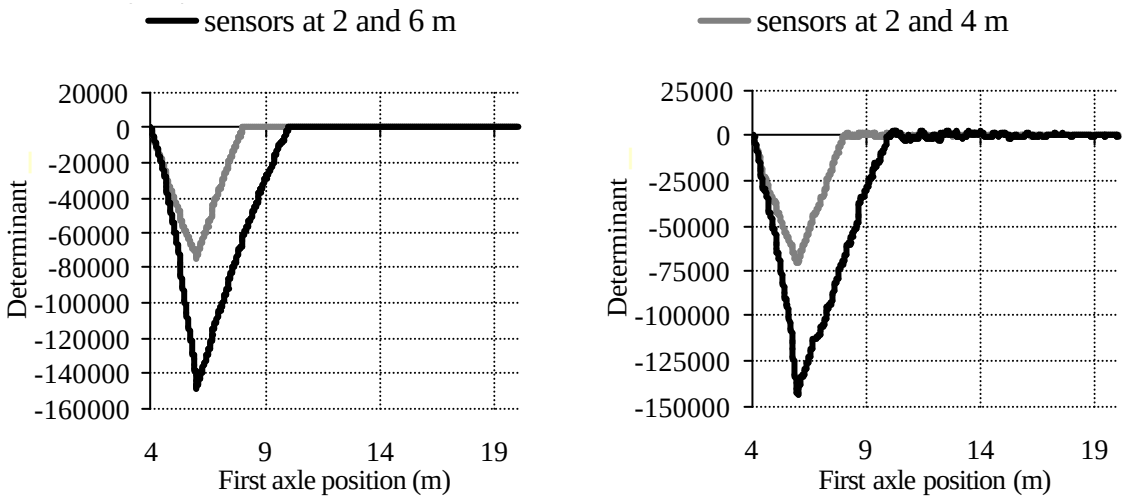

(a) Determinant by static MS-BWIM

(b) Determinant by dynamic MS-BWIM

Figure 7.20 (continued on following page)

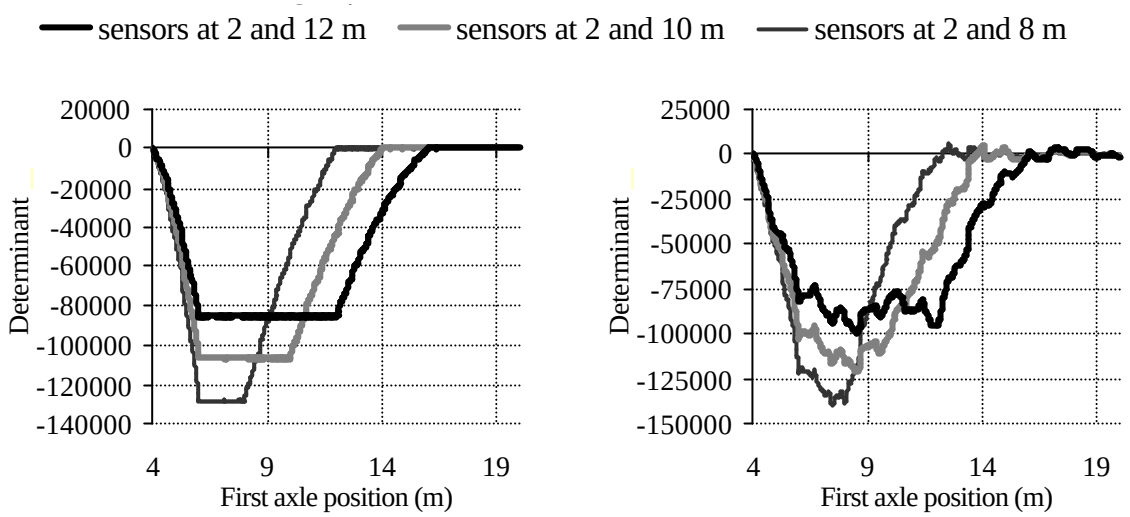

(c) Determinant by static MS-BWIM (d) Determinant by dynamic MS-BWIM

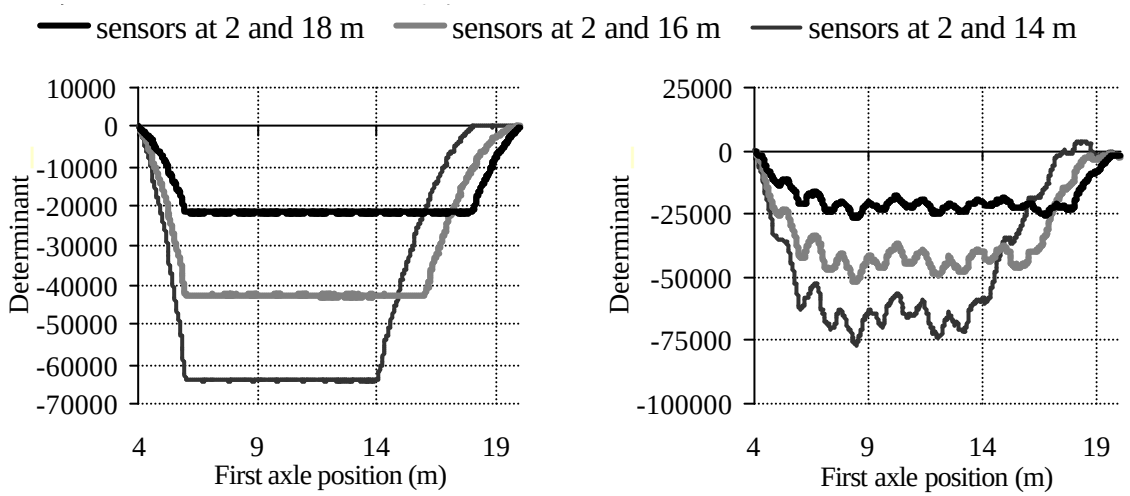

(e) Determinant by static MS-BWIM (f) Determinant by dynamic MS-BWIM

Figure 7.20 – Values of determinant for different combinations of two sensors

If a minimum number of sensors is chosen (this is, same as number of axles: 2 in this case), solution is only possible in a fixed portion of the bridge. Instantaneous axle calculations by a static and dynamic MS-BWIM are represented in Figures 7.21 and 7.22 for the front and rear axles respectively. If using two sensors, instantaneous calculation is feasible in those sections of the bridge where the determinant is high enough. The maximum value of this determinant generally takes place when the vehicle is between both sensors (the exact location depends on the influence line and the axle spacing) and it becomes zero when the vehicle moves away from this space between them. Thus, when using sensors at 2 and 4 m, instantaneous axle values can only be obtained before the first axle reaches 7 m from the start of the bridge. If using sensors at 2 and 6 m, calculations can be further extended to 9 m.

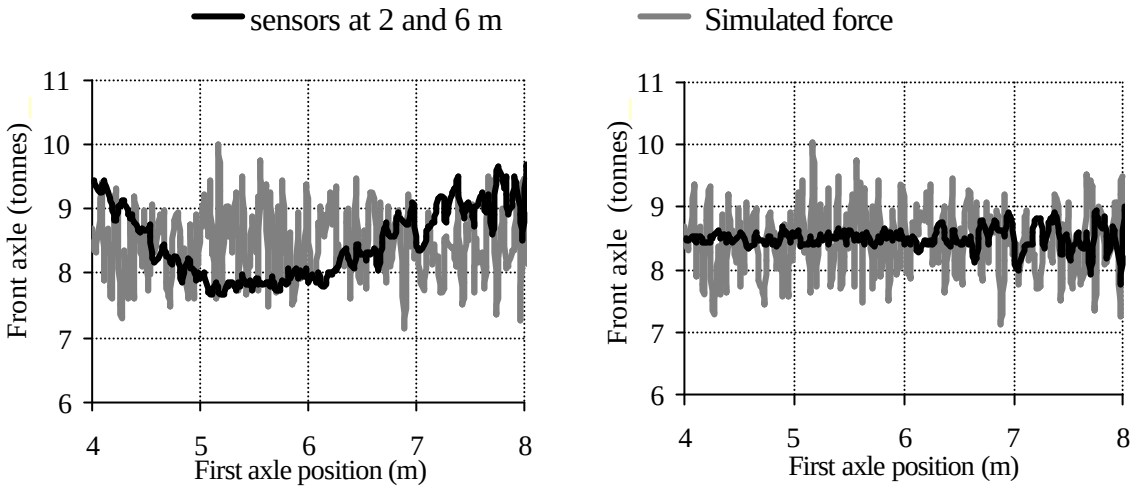

(a) Static MS-BWIM (at 2 and 6 m) (b) Dynamic MS-BWIM (at 2 and 6 m)

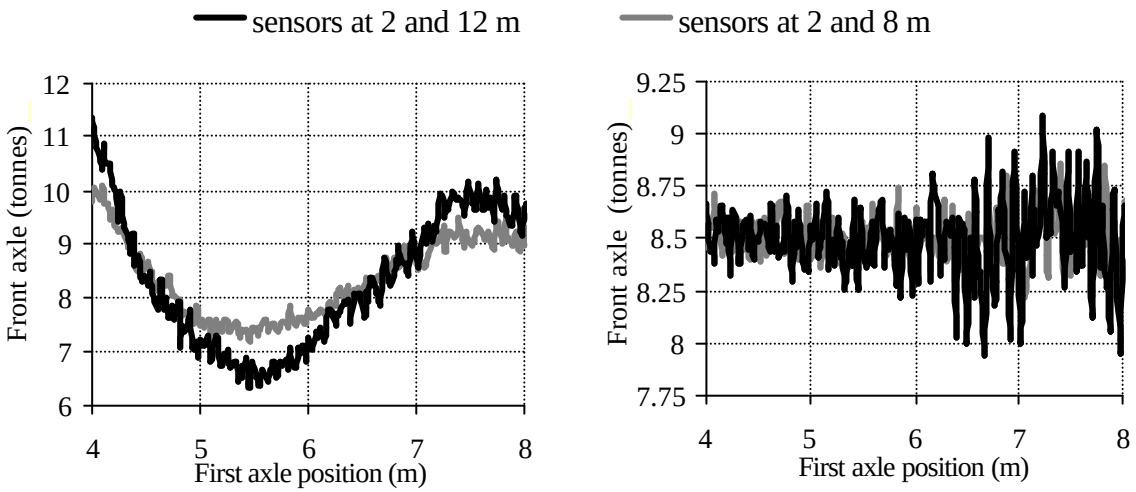

(c) Static MS-BWIM (at 2, 8 and 12 m) (d) Dynamic MS-BWIM (at 2, 8 and 12 m)

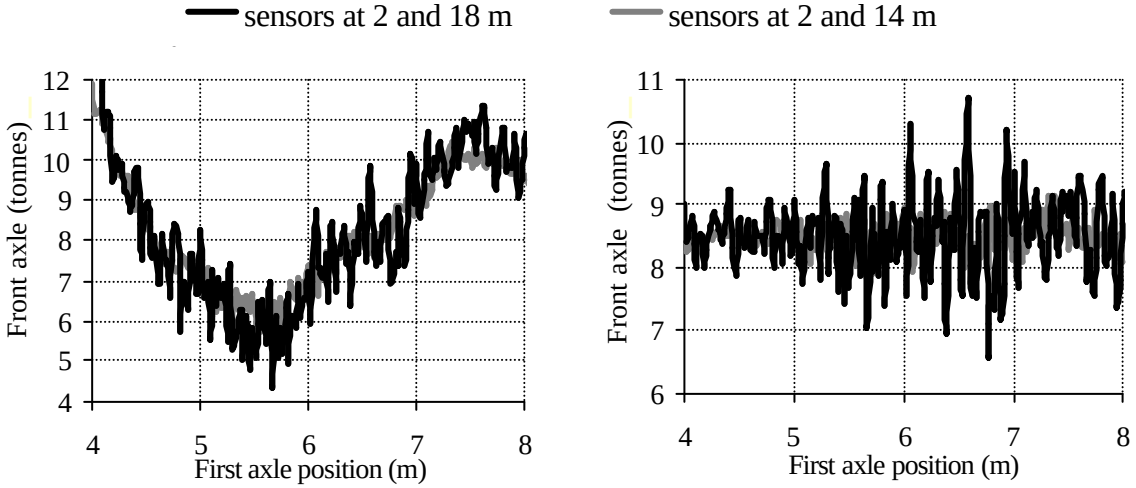

(e) Static MS-BWIM (at 2, 14 and 18 m) (f) Dynamic MS-BWIM (at 2, 14 and 18 m)

Figure 7.21 – Instantaneous calculation of front axle weight for combinations of 2 sensors

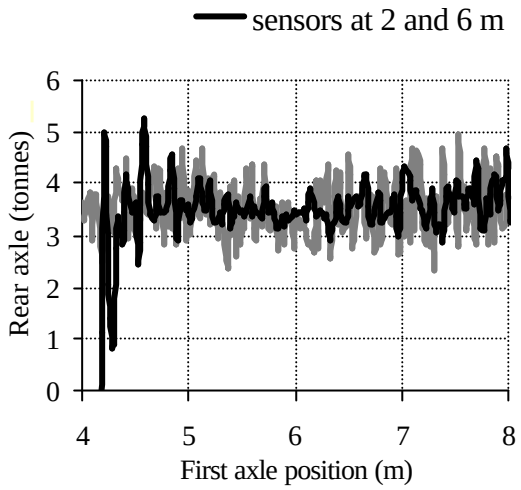

(a) Static MS-BWIM (at 2 and 6 m)

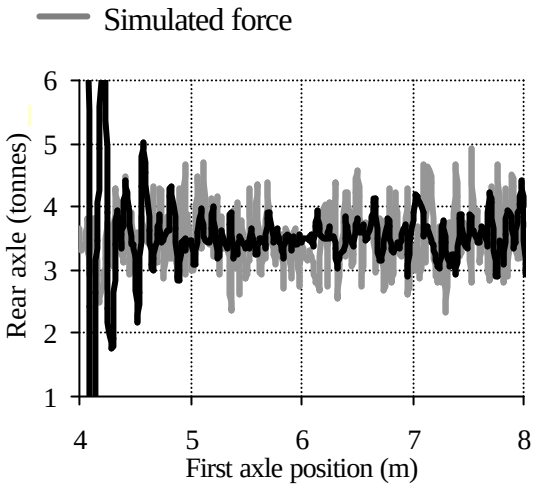

(b) Dynamic MS-BWIM (at 2 and 6 m)

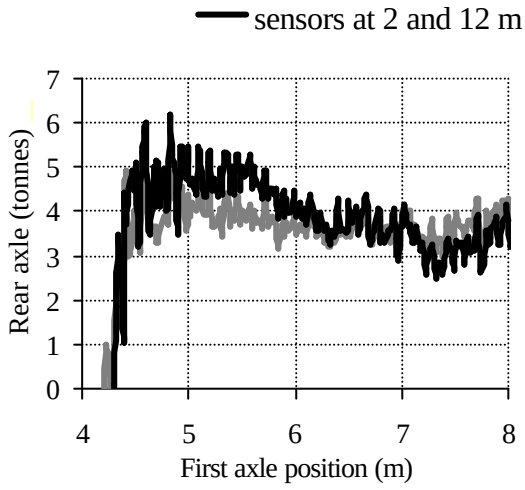

(c) Static MS-BWIM (at 2, 8 and 12 m)

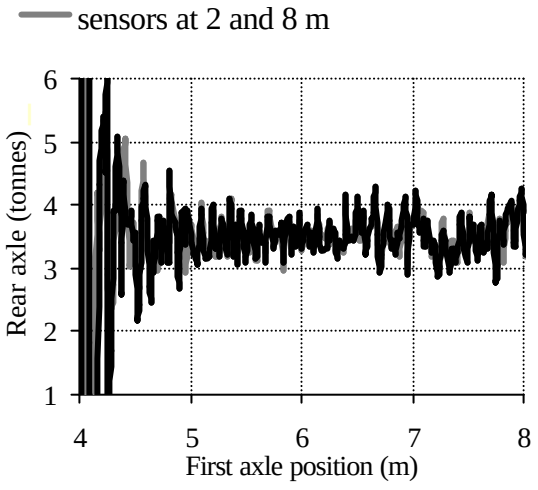

(d) Dynamic MS-BWIM (at 2, 8 and 12 m)

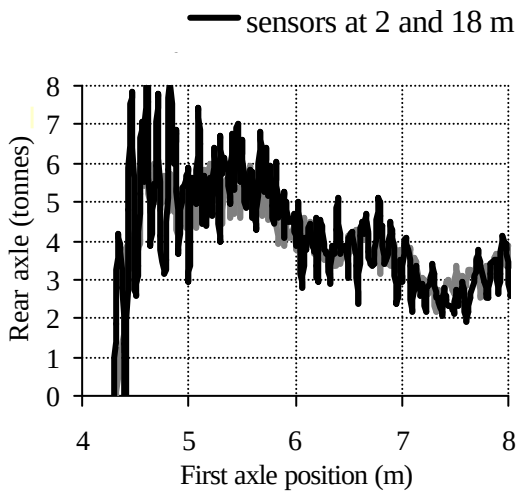

(e) Static MS-BWIM (at 2, 14 and 18 m)

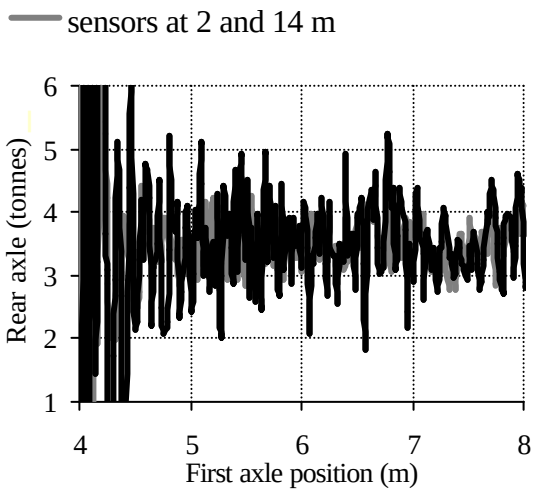

(f) Dynamic MS-BWIM (at 2, 14 and 18 m)

Figure 7.22 – Instantaneous calculation of rear axle weight for combinations of 2 sensors

The criterion to stop calculations can be established by the instant when the root mean square of the axle history tends towards infinity. Figure 7.23 represents the root mean square of accumulated instantaneous calculations by the dynamic MS-BWIM algorithm in Figure 7.21.

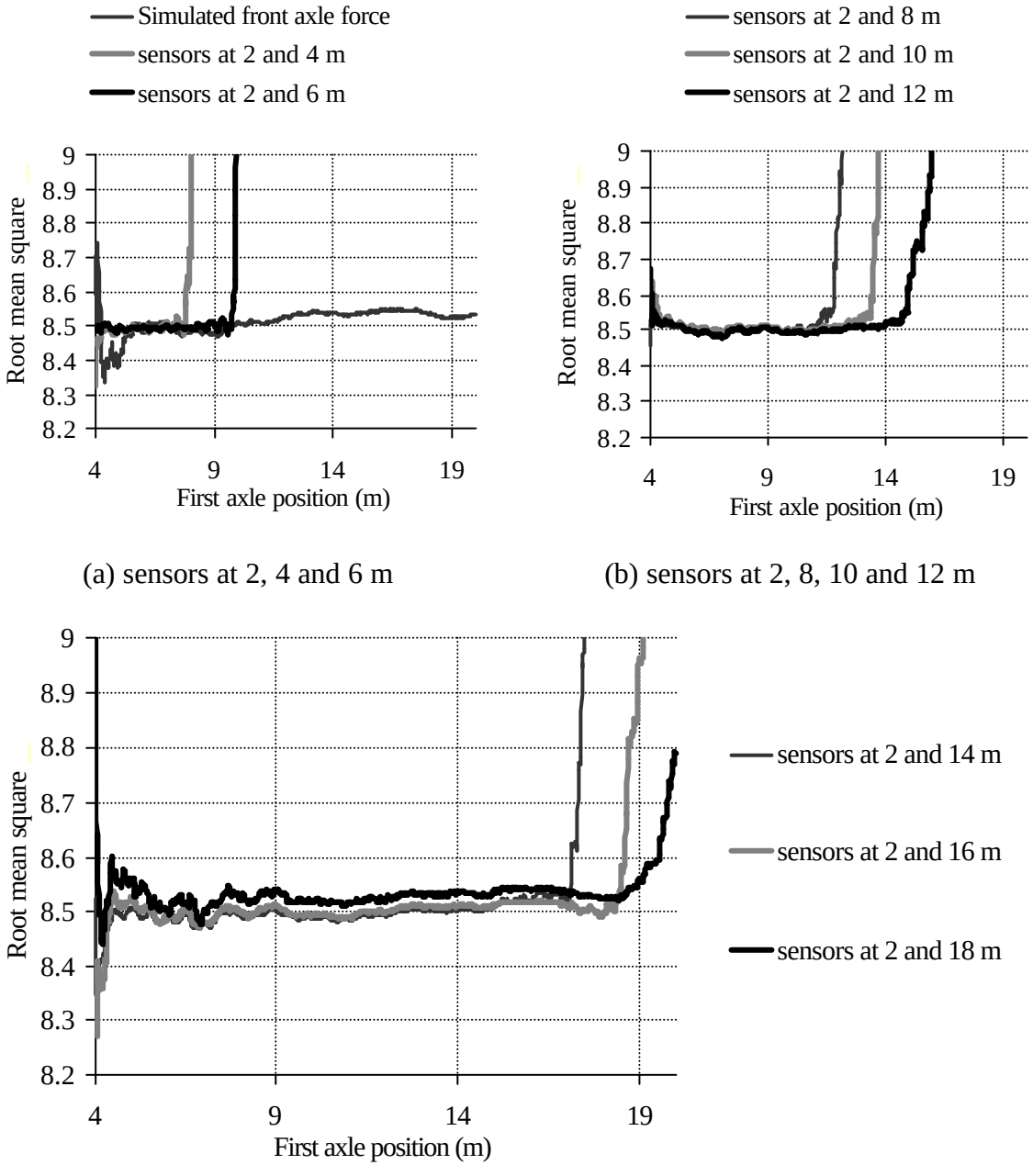

(a) sensors at 2, 4 and 6 m

(b) sensors at 2, 8, 10 and 12 m

(c) sensors at 2, 14, 16 and 18 m

Figure 7.23 – Values of root mean square for front axle and combinations of 2 sensors

A longer force-time history could be obtained by using sensors at both ends of the bridge. However, for a simply supported bridge, strain in locations close to the bridge supports is

small and hence, it is not very sensitive to changes in traffic loads. Some combinations of sensors give null determinant or very small values (prone to numerical instability) as shown in Figure 7.24. Sensors at 6 and 16 m could achieve a reasonable result along most of the bridge length.

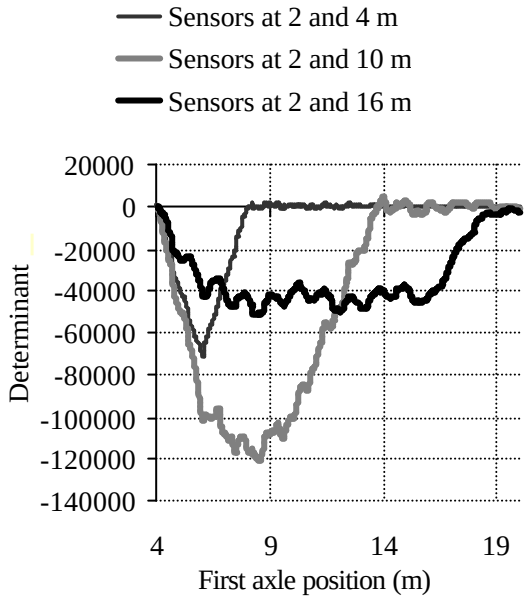

(a) Sensors at 2, 4, 10 and 16 m

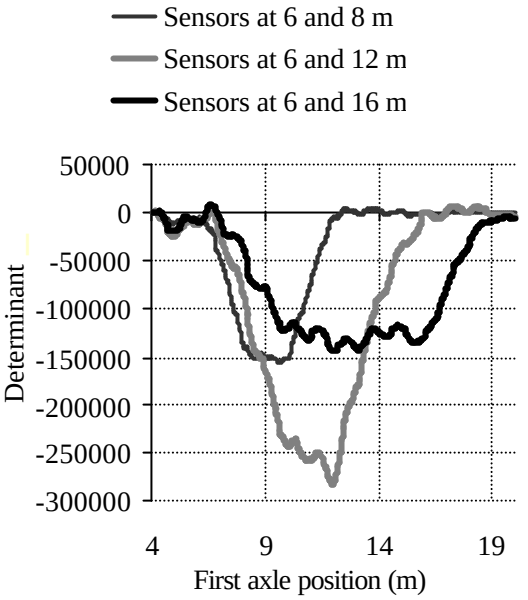

(b) Sensors at 6, 8, 12 and 16 m

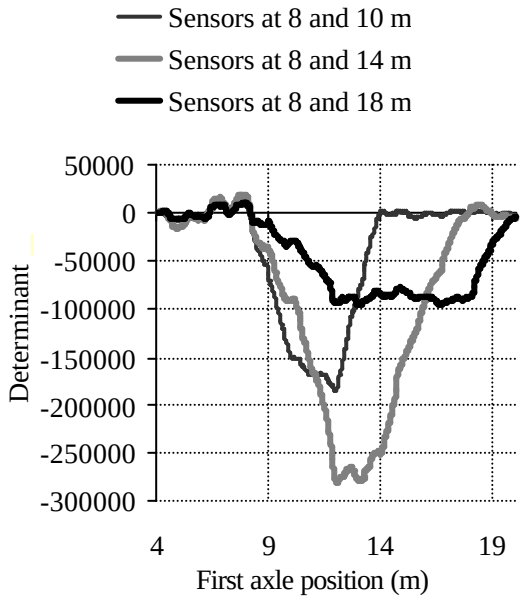

(c) Sensors at 8, 10, 14 and 18 m

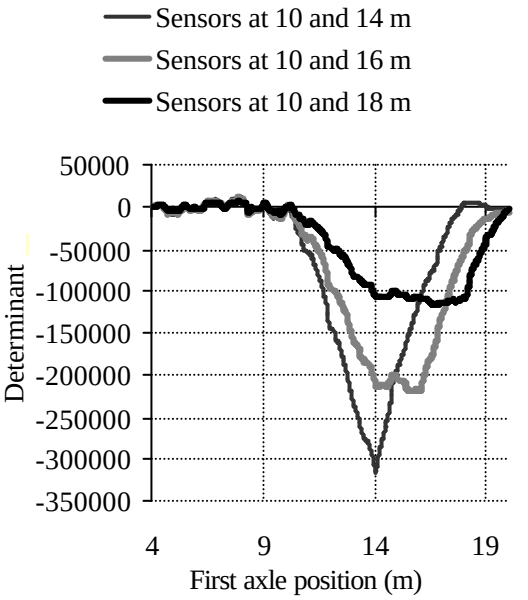

(d) Sensors at 10, 14, 16 and 18 m

Figure 7.24 – Values of determinant for different combination of two sensors and dynamic MS-BWIM algorithm

The main shortcoming of this approach arises from considering truck configurations of 3 or more axles. Then, the determinant becomes zero along most of the bridge, regardless of the combination of sensors used for the calculation. Figure 7.25 illustrates the value of the determinant obtained by the static MS-BWIM algorithm if using combinations of 3 sensors (this is the minimum number required to solve a 3-axle truck).

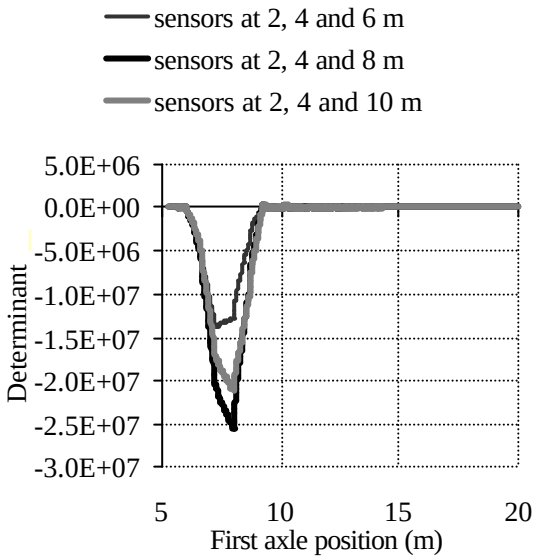

(a) sensors at 2, 4, 6, 8 and 10 m

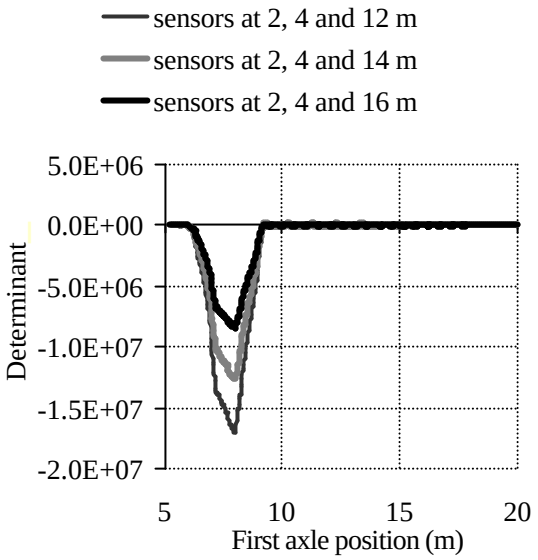

(b) sensors at 2, 4, 12, 14 and 16 m

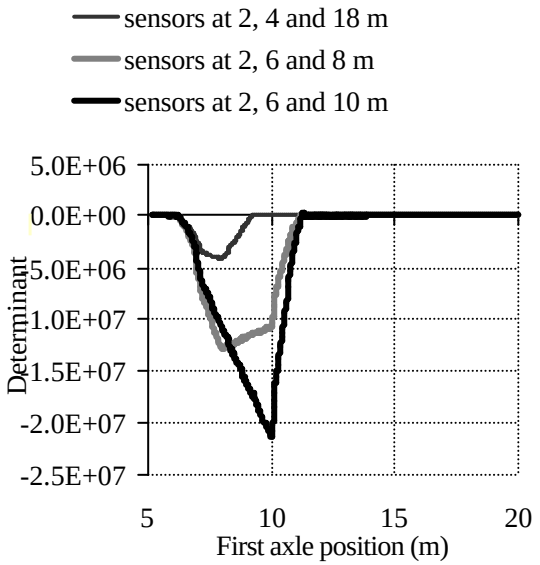

(c) sensors at 2, 4, 6, 8, 10 and 18 m

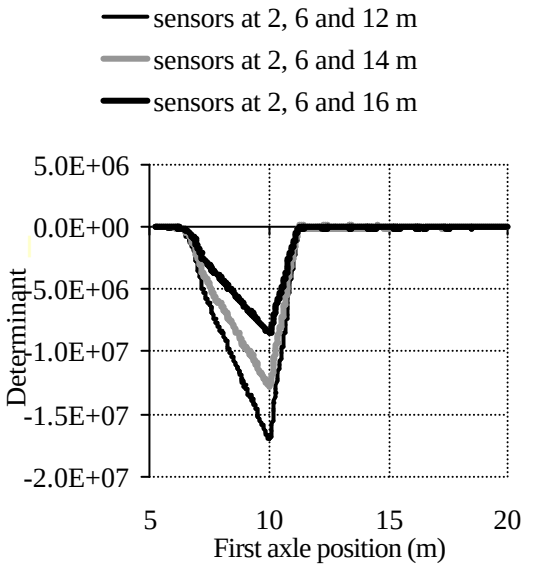

(c) sensors at 2, 6, 12, 14 and 16 m

Figure 7.25 – Values of determinant for combinations of 3 sensors

Figure 7.26 shows the value of the determinant obtained by the static and dynamic MS-BWIM algorithms if using combinations of 4 sensors (minimum number to solve the presence of 4 axles on the bridge). In either case, as the number of axles increases, the bridge length where solution is feasible, decreases.

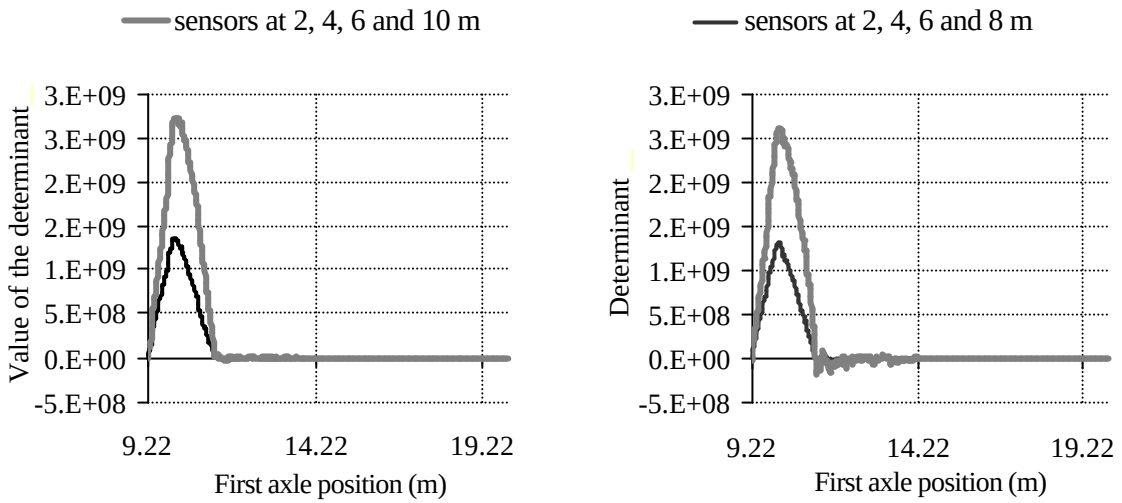

(a) Static MS-BWIM (b) Dynamic MS-BWIM

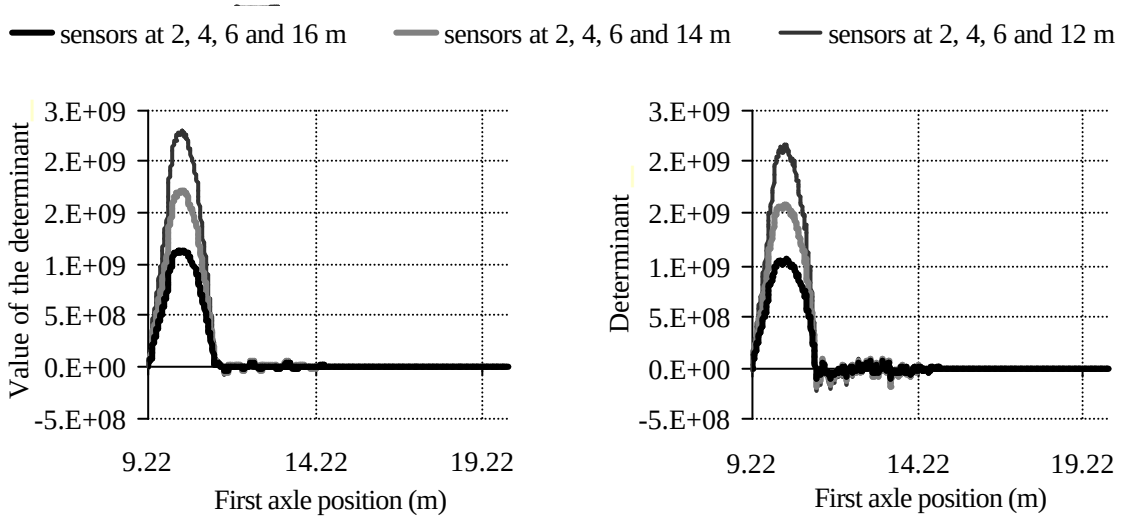

(a) Static MS-BWIM (b) Dynamic MS-BWIM

Figure 7.26 (continued on following page)

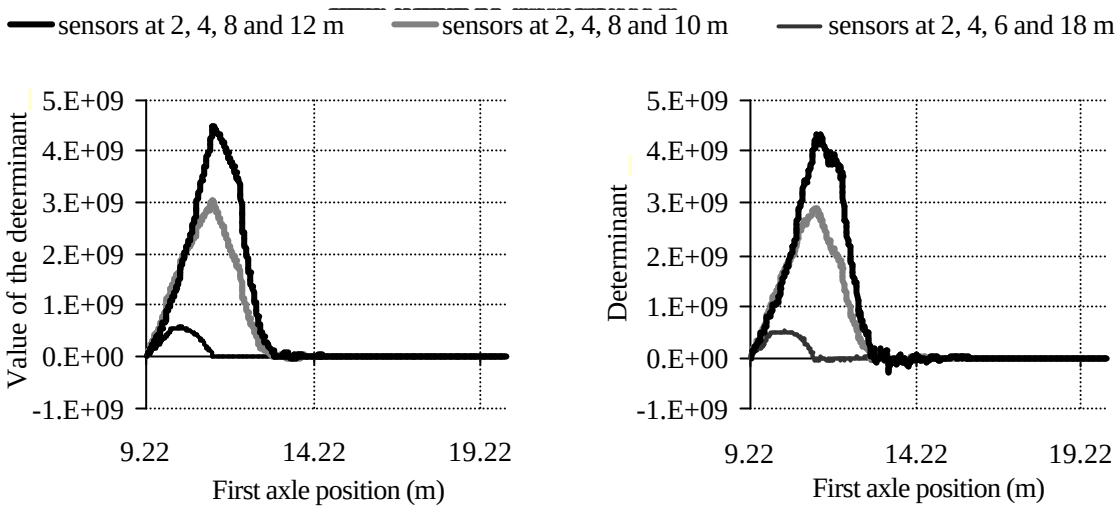

(a) Static MS-BWIM (b) Dynamic MS-BWIM

Figure 7.26 – Values of determinant for combinations of 4 sensors

If using more sensors and a least squares fitting technique, it is possible to solve for a higher number of axles and the length where solution is possible increases. This instantaneous calculation along the length of the bridge requires a lot of sensors, well in excess of the number of axles. If there are a number of sensors, *m*, equal or greater than the number of axles *n*, it is possible to minimise the error function defined in Equation 7.31:

$$f = \sum_{k=1}^{k=m} (\varepsilon_k - \tilde{\varepsilon}_k)^2 \quad \text{at each instant } t \tag{7.31}$$

where ε_k is the theoretical total strain due to the applied load at location k and $\tilde{\varepsilon}_k$ is the measured strain due to the applied load at location k.

By assuming linearity and applying the principle of superposition, it is possible to express the strain at each sensor as:

$$\varepsilon_k = \varepsilon_{k1} W_1 + \varepsilon_{k2} W_2 + \ldots + \varepsilon_{kn} W_n \tag{7.32}$$

By combining Equations 7.31 and 7.32:

$$f = \sum_{k=1}^{k=m} (\varepsilon_{k1} W_1 + \varepsilon_{k2} W_2 + ... + \varepsilon_{kn} W_n - \tilde{\varepsilon}_k)^2 \text{ at each instant } t \tag{7.33}$$

Differentiating Equation 7.33 with respect to the axle weight, W_i and setting it equal to zero gives:

$$\frac{df}{dW_i} = 2\sum_{k=1}^{k=m} (\varepsilon_{k1} W_1 + \varepsilon_{k2} W_2 + ... + \varepsilon_{kn} W_n - \tilde{\varepsilon}_k)\varepsilon_{ki} = 0 \tag{7.34}$$

The full set of equations can be expressed in matrix form as:

$$\begin{bmatrix} \sum_{k=1}^{k=m} \varepsilon_{k1}\varepsilon_{k1} & \sum_{k=1}^{k=m} \varepsilon_{k2}\varepsilon_{k1} & . & \sum_{k=1}^{k=m} \varepsilon_{kn}\varepsilon_{k1} \\ \sum_{k=1}^{k=m} \varepsilon_{k1}\varepsilon_{k2} & \sum_{k=1}^{k=m} \varepsilon_{k2}\varepsilon_{k2} & . & \sum_{k=1}^{k=m} \varepsilon_{kn}\varepsilon_{k2} \\ . & . & . & . \\ \sum_{k=1}^{k=m} \varepsilon_{k1}\varepsilon_{kn} & \sum_{k=1}^{k=m} \varepsilon_{k2}\varepsilon_{kn} & . & \sum_{k=1}^{k=m} \varepsilon_{kn}\varepsilon_{kn} \end{bmatrix} \begin{Bmatrix} W_1 \\ W_2 \\ . \\ W_n \end{Bmatrix} = \begin{Bmatrix} \sum_{k=1}^{k=m} \tilde{\varepsilon}_k \varepsilon_{k1} \\ \sum_{k=1}^{k=m} \tilde{\varepsilon}_k \varepsilon_{k2} \\ . \\ \sum_{k=1}^{k=m} \tilde{\varepsilon}_k \varepsilon_{kn} \end{Bmatrix} \tag{7.35}$$

where:

$\tilde{\varepsilon}_k$: measured strain due to the total applied load at sensor location k,

ε_{ij} : theoretical strain at sensor location i due to moving load located at j (influence line in the static approach, or dynamic response due to a unit load in the dynamic case),

W_j : applied load at location j,

n : total number of axles on the bridge.

Finally, applied loads (weights) can be calculated from Equation 7.36:

$$\{W\}_{nx1} = [\varepsilon]_{nxn}^{-1} \{\tilde{\varepsilon}\}_{nx1} \tag{7.36}$$

If the number of strain sensor locations is high enough, Equation 7.36 provides a solution along most of the bridge. The static value can be obtained from the root mean square of the calculated instantaneous axle forces.

The value of the determinant $|e|$ at each instant for a 2-axle truck on a 20 m simply supported bridge with sensors spaced every 2 m is shown in Figure 7.27. This determinant has been obtained using the static equations illustrated in Figure 7.19 and the dynamic reference of 7.16.

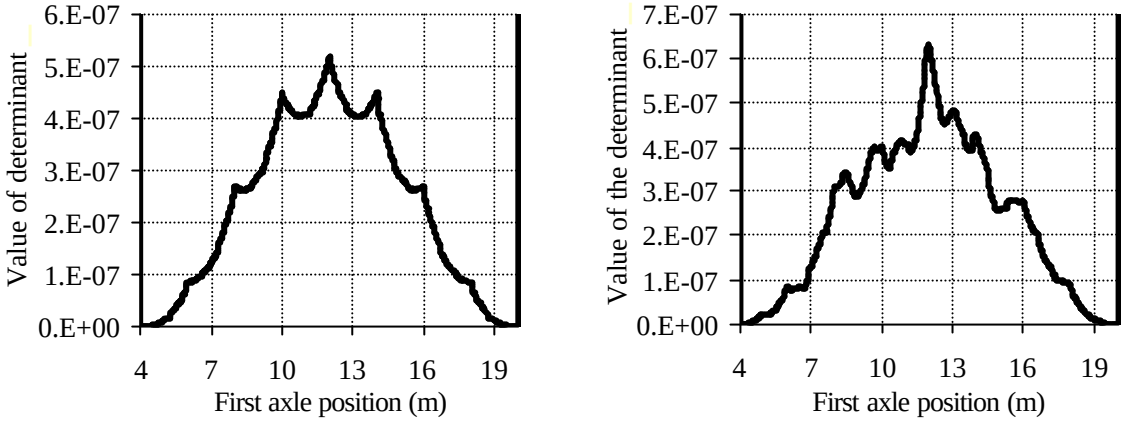

(a) Static MS-BWIM (b) Dynamic MS-BWIM

Figure 7.27 – Values of determinant $|e|$ for each position of a 2-axle vehicle

Figure 7.28 shows the value of the determinant for a 3 and 4-axle truck respectively during the time all axles are on the bridge. Both static and dynamic multiple-sensor approaches (Figure 7.28) are able to achieve an instantaneous calculation for the time that the vehicle is on the bridge. Unlike the 'static' determinant, the 'dynamic' determinant is not symmetric.

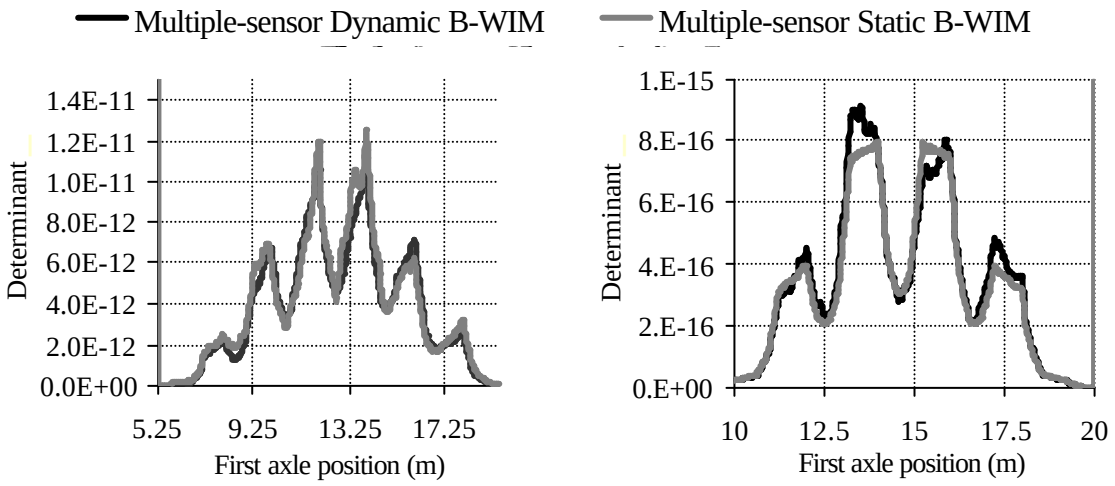

(a) 3-axle vehicle (b) 4-axle vehicle

Figure 7.28 – Values of determinant $|e|$ for 3 and 4-axle vehicles

Figure 7.29 shows the differences between the representation of the axle load history obtained by the two multiple-sensor Bridge WIM algorithms in the case of the front axle of a moving 2-axle body vehicle. Equation 7.36 has been used for this instantaneous calculation.

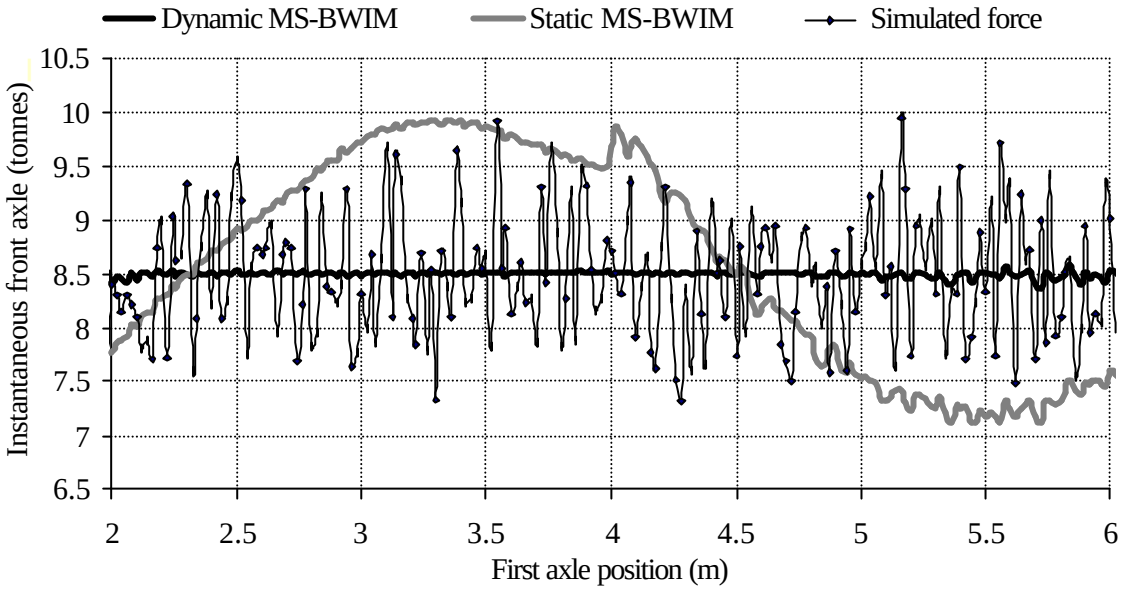

Figure 7.29 – Applied axle load calculated by 2 different multiple-sensor approaches using a least square fitting technique at each instant

The multiple-sensor systems are not able to reproduce the instantaneous applied axle forces accurately, but the dynamic system gives results around the real static weight of 8.5 tonnes along most of the bridge length. Figure 7.30 represents the whole load history of this front axle, the rear axle (static value = 3.5 tonnes) and the GVW (12 tonnes) by both multiple-sensor approaches. The estimation of instantaneous forces does not appear to be very accurate. However, the average value along the bridge can be very close to the static value if the number of readings is high enough (in particular for the static approach). The start and end of the instantaneous calculation should be avoided due to obvious rounding errors. A dynamic B-WIM algorithm based on one longitudinal location (as presented in Section 7.3) might be able to predict static weights as accurately as the multiple-sensor approach.

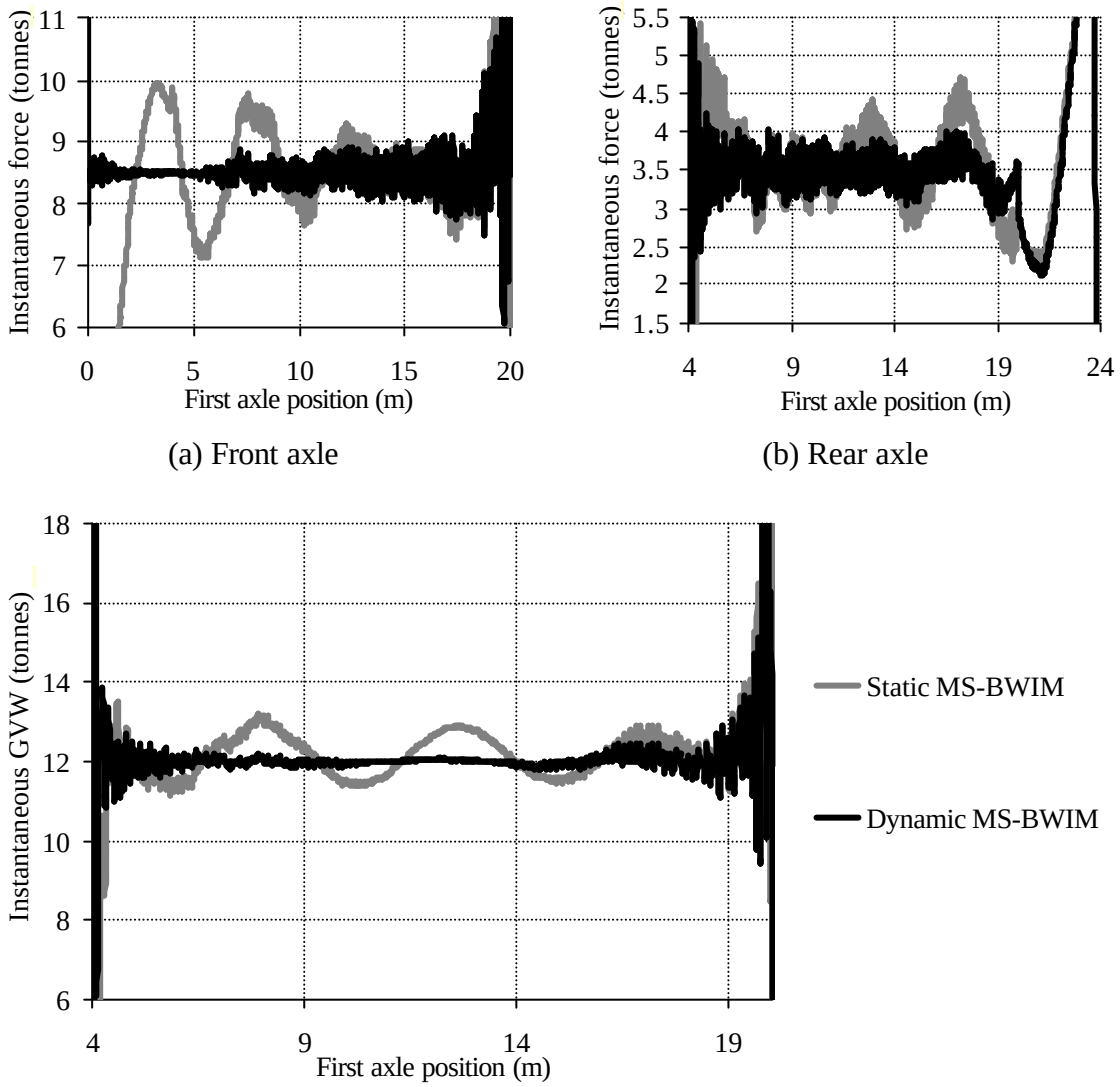

(a) Front axle

(b) Rear axle

(c) Gross Vehicle Weight

Figure 7.30 – Instantaneous forces by a multiple-sensor BWIM algorithm

7.5.3 An Algorithm based on Modal Decoupling

The approach described in this section uses strain gauges at different longitudinal locations to obtain a number of independent measurements of axle loads at each point in time. The steps involved in this dynamic algorithm based on modal decoupling are: (a) compute natural frequencies and mode shapes for the bridge, (b) calculate contribution of each mode shape from strain readings, (c) solve dynamic equation to obtain generalised load associated with each mode shape and finally (d) evaluate axle loads and gross vehicle weights from generalised load. Compared to the dynamic algorithm developed by Dempsey (Section 3.6.3), there are some improvements concerning:

- A better evaluation of the strain dynamics
- A greater number of mode shapes
- A description of the evolution of the axle load with time

(a) Compute mode shapes and frequencies

The beam displacements in a dynamic situation can be represented by:

$$z(x,t) = \sum_{i=1}^{\infty} \phi_i(x) Z_i(t) \tag{7.37}$$

where $\phi_i(x)$ represents the shape of the i^{th} mode shape, and $Z_i(t)$ represents the variation of amplitude with time of the i^{th} mode.

For a simply supported beam:

$$\phi_i(x) = \sin\left(\frac{i\pi x}{L}\right) \tag{7.38}$$

and then, the deflection is given by substituting 7.38 in 7.37:

$$z(x,t) = \sum_{i=1}^{\infty}\left[\sin\left(\frac{i\pi x}{L}\right) Z_i(t)\right] \tag{7.39}$$

And the bending moment is:

$$M(x,t) = EI\frac{\partial^2 z(x,t)}{\partial x^2} \tag{7.40}$$

By combining Equations 7.40 and 7.39:

$$M(x,t) = -EI\sum_{i=1}^{\infty}\left[\left(\frac{i\pi}{L}\right)^2 \sin\left(\frac{i\pi x}{L}\right) Z_i(t)\right] \tag{7.41}$$

Hence, bending moment can be expressed as a linear function of a series of mode shapes with amplitude $Z_i(t)$ that depends on time.

(b) Calculate contribution of each mode shape from strain readings

From Equation 7.41, measured bending strain in a particular location will be given by:

$$\varepsilon(x,t) = c\sum_{i=1}^{\infty}\left[\left(\frac{i\pi}{L}\right)^2 \sin\left(\frac{i\pi x}{L}\right) Z_i(t)\right] \tag{7.42}$$

where c is a constant. If there are strain sensors in m different longitudinal positions, it is possible to know the contribution Z_i of m mode shapes at each instant. A number of sensors higher than the number of mode shapes is required (solution through a least squares fitting technique).

The constants defining the contribution of each shape can be determined by positioning a stationary pre-weighed truck on the bridge: dynamic interaction is nil and the theoretical contribution of each mode shape can be obtained from the static bending moment diagram for that location. Once the constant for each sensor location is known, the amplitude Z_i for each shape ϕ can be derived from the strain readings for any truck at each point in time.

In matrix form:

$$\{\varepsilon\}_{mx1} = c\left[\frac{\partial^2 \phi}{\partial x^2}\right]_{mxm} \{Z\}_{mx1} \tag{7.43}$$

$$\therefore \{Z\}_{mx1} = \frac{1}{c}\left[\frac{\partial^2 \phi}{\partial x^2}\right]^{-1}_{mxm} \{\varepsilon\}_{mx1} \tag{7.44}$$

(c) Solve dynamic equation to obtain generalised load

The values of amplitudes $Z_i(t)$ obtained in step (b) are substituted in the generalised equations of motion to obtain generalised loads. Hence, the dynamic equations for each mode shape are:

$$d^2Z_i(t)/dt^2 + 2\xi_i\omega_i(dZ_i(t)/dt) + \omega_i^2 Z_i(t) = P_i(t)/M_i \qquad (7.45)$$

where $M_i = \int \phi_i^2(x)m(x)dx$, and $m(x)$ is mass per unit length. $m(x)$ can be calculated during calibration if it can be assumed to be constant along the bridge. Natural frequencies (ω_i) and damping ratio (ξ_i) are determined through a Fourier analysis of a sample strain record in free vibration. Modal loads $P_i(t)$ are obtained from Equation 7.45. These generalised loads are a function of the magnitude and position of every axle load for each mode shape.

(d) Evaluate axle loads and Gross vehicle weight

The generalized load $P_i(t_1)$ (obtained in step (c)) associated with the mode shape $\phi_i(x)$ at a certain time t_1 is given by:

$$\begin{aligned} P_i(t_1) &= \int_0^L \phi_i(x)\, W(x^1,t_1)]dx \\ &= \Sigma_r[\, \phi_i(x_r)W_r(x_r^1,t_1)] \end{aligned} \qquad (7.46)$$

where $W_r(x_r^1,t_1)$ is the axle load r in the position x_r^1 at time t_1. That is, for a n-axle truck and m-mode shapes used in the calculation:

$$\begin{aligned} &\phi_1(x_1^1)\, W_1(x_1^1,t_1) + \phi_1(x_2^1)W_2(x_2^1,t_1) + \ldots + \phi_1(x_n^1)W_n(x_n^1,t_1) = P_1(t_1) \\ &\phi_2(x_1^1)\, W_1(x_1^1,t_1) + \phi_2(x_2^1)W_2(x_2^1,t_1) + \ldots + \phi_2(x_n^1)W_n(x_n^1,t_1) = P_2(t_1) \\ &\text{----------} \\ &\phi_m(x_1^1)\, W_1(x_1^1,t_1) + \phi_m(x_2^1)W_2(x_2^1,t_1) + \ldots + \phi_m(x_n^1)W_n(x_n^1,t_1) = P_m(t_1) \end{aligned} \qquad (7.47)$$

Adding the above equations gives:

$$[\Sigma\phi_i(x_1^1)]^* W_1(x_1^1,t_1) + [\Sigma\phi_i(x_2^1)]^*W_2(x_2^1,t_1) + \ldots + [\Sigma\phi_i(x_n^1)]^*W_n(x_n^1,t_1) = \Sigma P_i(t_1) \qquad (7.48)$$

The calculation of the applied dynamic axle load $W_r(t)$ requires a number of mode shapes equal or greater than the number of axles (those ones of greater contribution $P_i(t)$ to the total load). In matrix form:

$$[\phi]_{mxm}\, \{W\}_{mx1} = \{P\}_{mx1} \qquad (7.49)$$

where $n = m$ is number of axles. Weights are then obtained through:

$$\{W\}_{mx1} = [f]_{mxm}^{-1} \{P\}_{mx1} \tag{7.50}$$

For short span bridges, the average of the varying axle load could be far from the static value. Static axle loads can be derived from the dynamic variation of axle load with time.

A simpler approach is to solve Equation 7.45 for just one mode shape (or a small number of them) and applying a least squares fitting method. This latter approach is expressed by minimising an error function defined by the squared difference between the measured record $S[P_i(t)]$ (Equation 7.45) and the predicted record. By rearranging the result of this derivative:

$$S_T[S_r[[Sf_i(x_r^t)]\ W_r(x_r^t,t)]\ Sf_i(x_s^t)] = S_T[SP_i(t)\ Sf_i(x_s^t)] \tag{7.51}$$

where $r = 1,2,..,m$ (number of axles), and $i = 1,2,\ldots,n$ (number of mode shapes). $Sf_i(x_s^t)$ is the value of the sum of the mode shapes corresponding to the position of the s^{th} axle at time t.

In matrix form:

$$[F^*]_{mxm}\ \{W\}_{mx1} = \{P^*\}_{mx1} \tag{7.52}$$

where $F^*_{rs} = S_T[Sf_i(x_r^t)Sf_i(x_s^t)]$, and $P_{s1}^* = S_T[SP_i(t)Sf_i(x_s^t)]$. Then, axle weights are given by:

$$\{W\}_{mx1} = [F^*]_{mxm}^{-1}\ \{P^*\}_{mx1} \tag{7.53}$$

If a number of mode shapes $n = 1$ is adopted, expressions 7.52 and 7.53 are as in Dempsey's algorithm (Section 3.6.3).

Finally, the gross vehicle weight would be given by:

$$GVW = W_1 + W_2 + \ldots + W_n \quad (7.54)$$

Even though a few mode shapes may define axle load accurately, when the contribution $Y_i(t)$ of each mode shape is calculated from measured strain in step (b), a much higher number of mode shapes is required; otherwise the results obtained in Equation 7.45 can be very poor. For a central dynamic loading, the first mode contribution provides over 98% of the central deflection, while 11 modes provide only about 97% of the total *bending moment* developed at midspan (Clough and Penzien 1975). In other words, accuracy in weight calculation increases when a higher number of longitudinal positions along the bridge is considered. This approach was the first attempt at a dynamic algorithm carried out by the author, but research was orientated in another direction due to the difficulties of implementation and testing on site (i.e. uncertainty in the modal components of the parameters, need for many sensors, etc…).

7.6 TWO-DIMENSIONAL MULTIPLE-SENSOR ALGORITHM

One-dimensional B-WIM algorithms generally add all strains obtained along the same longitudinal section to compensate for the influence of the transverse location of the truck. However, there will be differences in total strain for each path (Section 6.5.1). The magnitude of this difference will depend on the characteristics of the bridge. Even if the total bending of a bridge section is similar for different transverse locations, there is a need to deal with simultaneous traffic events. Though short span bridges might allow for one single vehicle at a time, there is always the possibility of another heavy vehicle travelling in the same or opposite direction in the adjacent lane. Hence, there is a need for a two-dimensional B-WIM algorithm. The algorithm presented in this section is a static algorithm that can be applied to simultaneous traffic events in the same or different lanes, at the same or different speeds.

The system uses influence lines due to a single wheel, instead of an axle weight. An advantage of predicting wheel weights is found in closely spaced axles. For instance, if all wheels have the same weight, the wheels closer to the strain sensor location will induce higher strain. This distinction is not possible if considering axle weights. The improvement in accuracy could be particularly significant in unbalanced trucks. The possibility of

representing the complete history of dynamic axle forces applied to the bridge can allow: the calculation of dynamic amplification factors, data for fatigue studies and data for investigations of spatial repeatability.

The algorithm is based on the same static equations as the multiple-sensor approach in Section 7.5.2 (Equations 7.31 to 7.35). This is an instantaneous calculation that allows a force-time history for each axle to be obtained. The difference is based on the definition of the influence line at each location. Hence, the bending moment $\mathring{a}_j$ at each sensor j due to p vehicles will be given by:

$$\boldsymbol{e}_j(x_j, y_j) = \frac{1}{E_j S_j} \sum_{i=1}^{p} W_{1i} I_j(x_i, y_i) + W_{2i} I_j(x_i \pm a_{1i}, y_i \pm d_i) + W_{3i} I_j(x_i \pm a_{1i} \pm a_{2i}, y_i \pm d_i) + \ldots \tag{7.55}$$

where W_{1i}, W_{2i}, … and a_{1i}, a_{2i}, … are wheel weights and axle spacings respectively corresponding to the i^{th} vehicle, d_i transverse distance between wheels, E_j and S_j the modulus of elasticity and section modulus at the sensor location j, I_j the influence line at sensor location j, (x_j,y_j) the position of the sensor j and (x_i,y_i) the position of the first axle of the vehicle.

An error function defined by the squared difference between measured $\tilde{\boldsymbol{e}}_j$ and theoretical strain $\mathring{a}_j$ at each sensor j is defined at each instant t:

$$f = \sum_{k=1}^{k=m} \left(\sum_{i=1}^{p} \sum_{j=1}^{n_i} \boldsymbol{e}_{kji} W_{ji} - \tilde{\boldsymbol{e}}_k \right)^2 \tag{7.56}$$

where n_i is the number of wheels of vehicle i, and $\mathring{a}_{kji}$ represents the value of the influence line at the sensor k for the location of wheel j in vehicle i.

By minimising Equation 7.56 with respect to the wheel weights:

$$\frac{df}{dW_{ji}} = 2 \sum_{k=1}^{k=m} \left(\sum_{i=1}^{p} \sum_{j=1}^{n_i} \boldsymbol{e}_{kji} W_{ji} - \tilde{\boldsymbol{e}}_k \right) \boldsymbol{e}_{kji} = 0 \tag{7.57}$$

In matrix form, wheel weights can be obtained at each instant from:

$$\{W\} = [e]^{-1} * \{\tilde{e}\} \tag{7.58}$$

where:

$$[e] = \begin{bmatrix} \sum_{k=1}^{k=m} e_{k11} e_{k11} & \sum_{k=1}^{k=m} e_{k21} e_{k11} & \cdot & \sum_{k=1}^{k=m} e_{knp} e_{k1p} \\ \sum_{k=1}^{k=m} e_{k11} e_{k21} & \sum_{k=1}^{k=m} e_{k21} e_{k21} & \cdot & \sum_{k=1}^{k=m} e_{knp} e_{k2p} \\ \cdot & \cdot & \cdot & \cdot \\ \sum_{k=1}^{k=m} e_{k1p} e_{kn_p p} & \sum_{k=1}^{k=m} e_{k2p} e_{kn_p p} & \cdot & \sum_{k=1}^{k=m} e_{kn_p p} e_{kn_p p} \end{bmatrix} \tag{7.59}$$

$$\{\tilde{e}_k\} = \begin{Bmatrix} \sum_{k=1}^{k=m} \tilde{e}_k e_{k11} \\ \sum_{k=1}^{k=m} \tilde{e}_k e_{k21} \\ \cdot \\ \sum_{k=1}^{k=m} \tilde{e}_k e_{kn_p p} \end{Bmatrix} \tag{7.60}$$

It is also proposed to optimise vehicle position at each instant, instead of assuming a uniform speed along the bridge as in all previous algorithms. If a pair of axle detectors is placed prior to the bridge, the information on axle spacing and speed can be used as initial values in the optimisation process shown in Figure 7.31. Once the vehicle is initially located on the bridge, the transverse and longitudinal positions are optimised as an extra pair of parameters besides axle forces. Initial values for wheel weights can be obtained by using a one-dimensional B-WIM algorithm as defined in previous sections. Axle weights can be assumed to be equally distributed between wheels in a first approach. Velocity and transverse locations are not assumed to be constant. Further, velocity is not a parameter of the objective function, but transverse and longitudinal co-ordinates of one of the front wheels. Instantaneous velocity is updated in every incremental step from these two co-ordinates. From the previous truck location and instantaneous velocity (re-calculated in each time step), it is possible to obtain initial values of transverse and longitudinal positions for the next incremental step. The parameters of the objective function are

changed in an iterative process and the solution is found when the change in their values is less than a specified tolerance. The parameters for positioning the truck are constrained in a reasonable area around the initial transverse and longitudinal positions. This area will depend on the scanning frequency and the maximum likely vehicle acceleration/deceleration.

The objective function is given by Equation 7.56. The parameters to be estimated at each incremental step are: longitudinal, x_i , and transverse location, y_i, for each truck i and wheel weights W_{ji}. Axle spacings could also be among these parameters, but only if values provided by road axle detectors give insufficient accuracy.

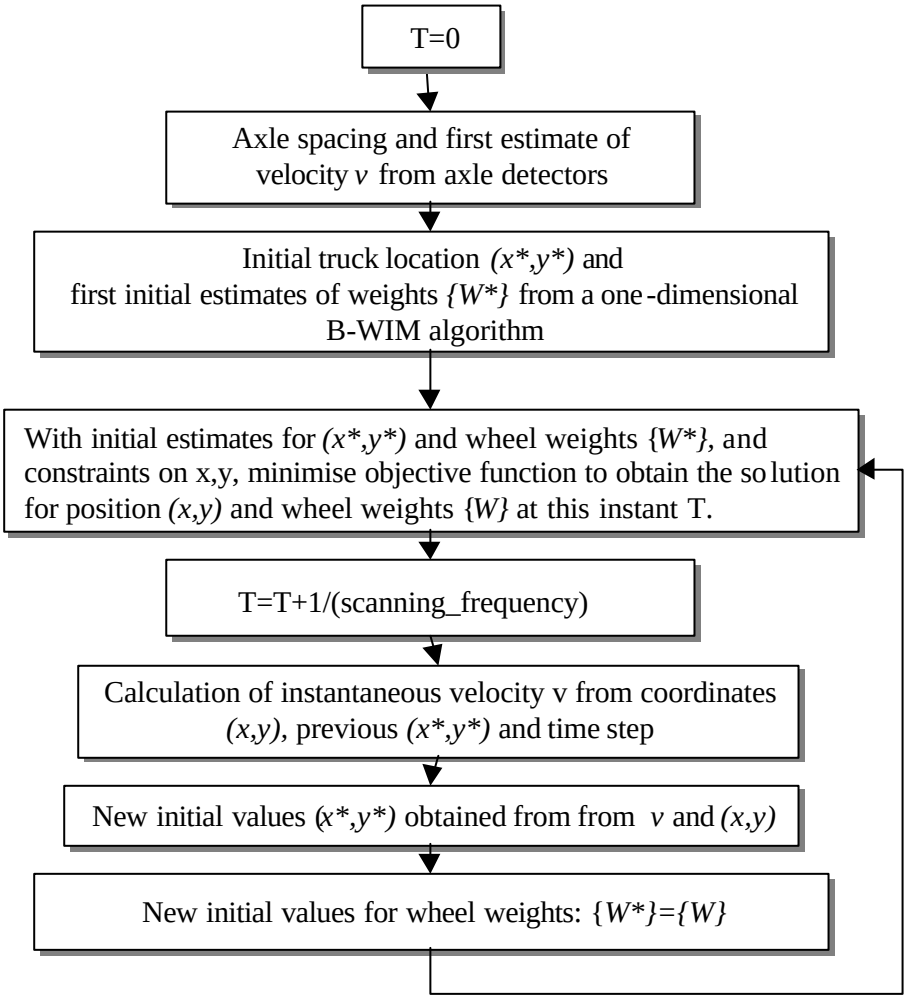

Figure 7.31 – Optimisation of two-dimensional instantaneous calculation

The disadvantage of this approach is the high number of sensors necessary to distinguish between the individual contribution of each wheel weight at each instant. The application of the algorithm is only recommended for short span bridges. A variant based on axle weights as parameters of the objective function (instead of using wheel weights) could be used for longer bridges. Compared to previous BWIM algorithms where an average speed parameter is optimised, the new algorithm optimises the vehicle position and re-calculate velocity in each time step.

7.7 SUMMARY

The search for a more accurate B-WIM algorithm has been focused on a consideration of dynamics. A new B-WIM algorithm that allows for bridge vibrations (natural frequencies, damping) has been presented (DB-WIM). More elaborate dynamic models can incorporate truck dynamics. The parameters of these models are determined by applying optimisation techniques to a number of measurement points. However, the randomness of these parameters (due to the high variety of truck and bridge mechanical characteristics) and the reduced information that can be obtained in the field, are a disincentive to using very refined dynamic models.

Static or dynamic equations can be formulated at more than one location. If the number of sensors is equal to or greater than the number of axles, the equations can be solved for the unknown axle weights for each instant in time. However, some of these equations could be dependent and a solution might not be achievable for all locations of the truck on the bridge. This is consistent with the original multiple-sensor B-WIM (MS-BWIM) system which was limited in the number of axles that could be weighed simultaneously (Kealy & O'Brien 1998). The author proposes a solution based on a least squares fitting technique that makes feasible the calculation of more axles.

An experimental algorithm based purely on the measured record is also introduced. This algorithm is based on the representation of the signal in the frequency domain. Weights are calculated from the spectrum. When the number of axles increases, the limiting frequency where spectra are compared might need to be increased and poor results have been obtained. However, the algorithm is calibrated in a way that can be directly applied to other algorithms based on the time domain. For instance, the method can be used

experimentally to obtain the influence line used in a static B-WIM algorithm or the dynamic answer due to a unit load used in DB-WIM.

The theoretical basis for a two-dimensional B-WIM algorithm has been established. This formulation takes into account the transverse location of the truck and the possibility of different trucks.

Finally, Table 7.1 identifies the main features of all the algorithms considered in this chapter. They all compare the measured strain to a theoretical strain. The difference lies in the theoretical strain used as reference.

Table 7.1 – B-WIM algorithms

Algorithm type	**Principle**
Spectral	Comparison of measured spectra at one sensor location to reference spectra in frequency domain.
Based on a bridge dynamic model	Comparison of measured strain at one sensor location to theoretical strain derived from a model that allows for bridge dynamics.
Based on a bridge + truck dynamic model	Comparison of measured strain at one or multiple bridge locations to theoretical strain derived from a model that allows for bridge-truck dynamic interaction.
Static multiple-sensor	Comparison of measured strains to theoretical static strain at different bridge locations.
Dynamic multiple-sensor	Comparison of measured strains at different bridge locations to theoretical strains derived from a model that allows for bridge dynamics.
Based on modal decoupling	Comparison of the estimation of the modal components of the applied force and the theoretical value derived from a bridge dynamic model.
Two-dimensional	Comparison of measured strains to theoretical static strain at different transverse and longitudinal bridge locations.

The first two algorithms (spectral and based on a bridge dynamic model) are based on measurements at only one longitudinal section. Average forces (assumed to be close to static weights) are calculated through a least squares fitting technique applied to all readings at the section location. The algorithm based on a bridge and truck dynamic model can be based on measurements at one or several sections. The solution is obtained through optimisation of an objective function in an iterative process. The other four algorithms (static multiple-sensor, dynamic multiple-sensor, based on modal decoupling and two-dimensional) are based on measurements at different sections. An instantaneous applied

force is obtained by applying a least squares fitting technique to the readings of all sensors at each instant. Then, static axle weights are derived from the corresponding load history.